Published in Journal of Contaminant Hydrology 91, issues 3-4, 203-232, 2007
which should be used for any reference to this work

Groundwater–surface water interaction and its role on TCE groundwater plume attenuation

Steven W. Chapman [a,*], Beth L. Parker [a], John A. Cherry [a], Ramon Aravena [a], Daniel Hunkeler [b]

[a] *Department of Earth Sciences, University of Waterloo, 200 University Avenue West, Waterloo, Ontario Canada N2L 3G1*
[b] *Centre for Hydrogeology, University of Neuchâtel, Rue Emile-Argand 11, CH-2007, Neuchâtel, Switzerland*

Abstract

A field investigation of a TCE plume in a surficial sand aquifer shows that groundwater–surface water interactions strongly influence apparent plume attenuation. At the site, a former industrial facility in Connecticut, depth-discrete monitoring along three cross-sections (transects) perpendicular to groundwater flow shows a persistent VOC plume extending 700 m from the DNAPL source zone to a mid-size river. Maximum TCE concentrations along a transect 280 m from the source were in the 1000s of μg/L with minimal degradation products. Beyond this, the land surface drops abruptly to a lower terrace where a shallow pond and small streams occur. Two transects along the lower terrace, one midway between the facility and river just downgradient of the pond and one along the edge of the river, give the appearance that the plume has strongly attenuated. At the river, maximum TCE concentrations in the 10s of μg/L and similar levels of its degradation product *cis*-DCE show direct plume discharge from groundwater to the river is negligible. Although degradation plays a role in the strong plume attenuation, the major attenuation factor is partial groundwater plume discharge to surface water (i.e. the pond and small streams), where some mass loss occurs via water–air exchange. Groundwater and stream mass discharge estimates show that more than half of the plume mass discharge crossing the first transect, before surface water interactions occur, reaches the river directly via streamflow, although river concentrations were below detection due to dilution. This study shows that groundwater and surface water concentration measurements together provide greater confidence in identifying and quantifying natural attenuation processes at this site, rather than groundwater measurements alone.

Keywords: Hydrogeology; Groundwater; Shallow aquifers; Discharge; Ponds; Streams; Rivers; Contaminant plumes; Solute transport; Trichloroethene; Natural attenuation; Carbon isotopes

* Corresponding author. Tel./fax: +1 506 454 2173.
E-mail address: swchapma@uwaterloo.ca (S.W. Chapman).

1. Introduction

Trichloroethene (TCE) is the most common groundwater contaminant in industrial areas (Stroo et al., 2003) and its attenuation under natural conditions in the groundwater zone has been the subject of many studies (e.g. Wiedemeier et al., 1999; NRC, 2000). Under favorable microbial and hydrogeochemical conditions in groundwater, TCE has been observed at some sites to strongly decline in concentration from high levels to levels that are within regulatory limits (NRC, 2000), which is the best circumstance for aquifers impacted by this or any contaminant. On the other hand, TCE also has been shown to be strongly conservative (e.g. Benker et al., 1997). At many sites, there is concern that contaminant migration will cause adverse impacts on water supplies or ecological systems. The literature indicates that many thousands of wells have been impacted by industrial volatile organic contaminants (VOCs) such as TCE (e.g. Squillace et al., 1999; Zogorski et al., 2006) and a National Priorities List study estimates that 51% of the identified 1218 hazardous waste sites, many of which include VOCs, impact surface waters (USEPA, 1991). Although the potential impact to surface water receptors is large, few published field studies focus on plumes discharging to them.

In non-arid regions, groundwater recharge commonly maintains the water table close enough to ground surface for the regional water table to closely follow the general shape of the topography (Tóth, 1962; Engelen and Kloosterman, 1996). Groundwater recharge in these regions typically ends up as groundwater discharge to surface water bodies (e.g. Winter et al., 1998; Winter, 1999). As groundwater approaches a surface water system such as a stream, the resulting flow system can be complex both physically and hydrogeochemically. The various ways that groundwater discharges and interacts with streams is described conceptually by Woessner (2000). As an extension of these conceptual flow models, combined with the strong internal variability of plume concentrations shown by Einarson and Mackay (2001) and Guilbeault et al. (2005), it is reasonable to expect that the nature of contaminant plumes completely or partially discharging to surface waters is also highly variable and complex.

The literature contains few field studies focused on plumes discharging to streams or rivers, and most of these focus monitoring primarily in the streambed. Examples where seepage meters and shallow piezometers have been used to examine the plume discharge into rivers include Norman et al. (1986), Avery (1994) and Hess et al. (1989), while plan-view distributions of VOCs in streambeds have been mapped using diffusion samplers (e.g. Vroblesky et al., 1991, 1996). There is an absence of well-documented studies in the literature where the natural attenuation of plumes, in cases where groundwater and surface water systems interact, is investigated in detail. Westbrook et al. (2005) studied a hydrocarbon plume discharging to an estuarine river using multiport wells along transects and drive point sampling below the river bed. Lorah and Olsen (1999) studied a VOC plume (TCE and PCA) discharging from an aerobic sand aquifer to a freshwater tidal wetland, showing evidence for strong anaerobic biodegradation during discharge through the organic-rich wetland sediments. Conant et al. (2004) provide one of the few well-documented examples of a VOC plume discharging to a surface water body, where PCE, originating from a dry cleaning site, discharges to a small river primarily in the form of its transformation products (TCE, *cis*-DCE and VC) with extensive biodegradation occurring within the top 2.5 m of the streambed and only minimal degradation upgradient in the aquifer. Although VOC concentrations discharging to the river were high, the river water showed only very low concentrations, a few 10s of μg/L at most and generally below detection, due to mixing (dilution) and loss to the atmosphere from the river. From the perspective of the river, the PCE and its transformation products were completely attenuated by dilution, but from the perspective of the

other components of the hydrologic system, natural attenuation by physical and degradation processes was weak.

This study, at a former industrial facility in Connecticut, focuses on investigations of a TCE plume originating from a DNAPL source zone in a shallow sand aquifer and ultimately discharging to a river. Previous monitoring using conventional wells showed large concentration declines between the source zone and river (i.e. apparent strong plume attenuation). The transect approach was applied with intensive monitoring of contaminant distribution in the aquifer using depth-discrete techniques along cross-sections orthogonal to groundwater flow for reliable assessment of maximum concentrations in the plume, and to be used with groundwater flux estimates for estimating changes in plume mass discharge along the plume flow path. A shallow pond and small tributary streams occur within the plume area upgradient of the river. The goal was to determine the trends in TCE and degradation products along the subsurface flow paths and also in the pond and streams at many locations to identify the mechanisms causing plume attenuation. The fate of the VOC mass in the various components of the hydrogeologic system was examined to determine why so little of the subsurface TCE mass emanating from the DNAPL source makes its way via the aquifer to the river (i.e. to document processes causing apparent strong plume attenuation). This is the first well-documented field study where the TCE mass originating at a subsurface DNAPL source has been tracked through a complex hydrologic system involving an aquifer connected to a pond, small streams and a river, each receiving a component of the plume mass discharge.

2. Site description

The site, located in Connecticut, was used for manufacturing of metal products from 1952 to 2001. TCE was the primary solvent used for degreasing until the early 1970s, and was stored in underground tanks at the east side of the facility (Fig. 1). Specific details concerning TCE spills are not known; however, TCE releases probably began shortly after the facility operations began, causing formation of a persistent DNAPL source zone at the bottom of the aquifer (Parker et al., 2003). The aquifer is underlain by a thick aquitard, which provides excellent protection of deeper aquifer deposits, and the extent of TCE transport into the aquitard suggests contamination began about 40 to 50 years ago (Parker et al., 2004) consistent with site history. Most of the DNAPL zone was isolated by a sheet piling enclosure in 1994 (keyed into the underlying aquitard), causing reduction in downgradient plume concentrations, although the plume persists largely due to back diffusion of mass from the aquitard to the aquifer (Chapman and Parker, 2005).

Figs. 1 and 2 show the site in map view and cross-section, respectively. The main building is situated on an upper terrace, with a steep embankment to the west transitioning to a lower terrace, which slopes gradually to a mid-size river (average annual streamflow of 299 cubic feet per second (cfs) or 7.3×10^8 L/day, Connecticut Department of Environmental Protection, http://dep.state.ct.us/wtr/watershed/wtshdmgtindex.htm). Groundwater flow in the surficial aquifer is generally to the west toward the river with an average hydraulic gradient of about 0.01, although much higher local gradients occur in the area of the embankment, with groundwater seeps evident in some areas near the base. Along the lower terrace, a shallow pond and small streams occur. The pond (Fig. 3), at the location of a former surface impoundment, is about 100 m long (perpendicular to groundwater flow) and 30 m wide, with a maximum depth of about 0.5 m. The pond has no surface inflows or outflows. Four streams (m-, x-, y- and z-) originate at outfalls near the base of the embankment, which received storm and melt water runoff from the facility, on-site wastewater treatment plant discharge and non-contact cooling water. Volumetric inputs to the

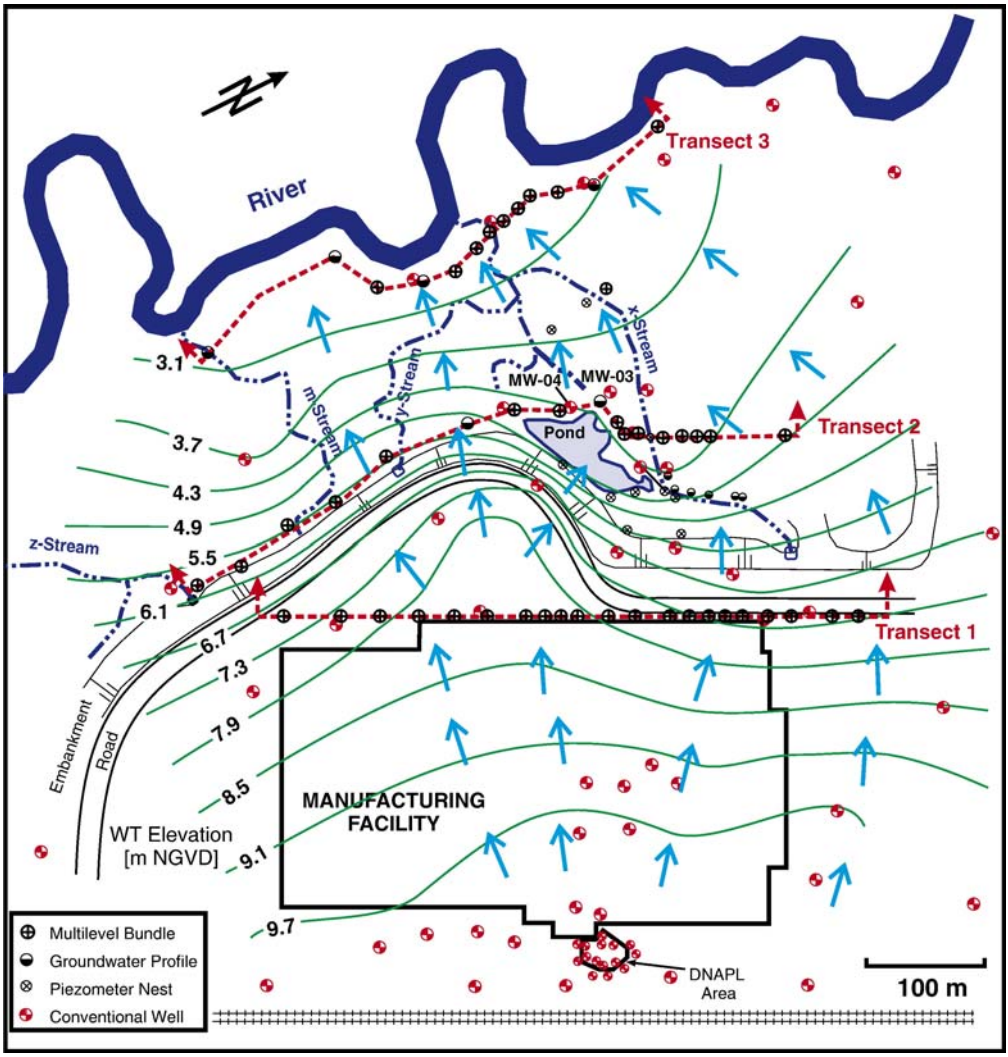

Fig. 1. Plan map showing locations of the DNAPL source zone and enclosure, building, monitoring transects, multilevel wells, Profiler locations, piezometer nests, selected conventional wells and surface water features (pond, streams, river). Water table contours are shown from a snapshot in September 1999, using several of the conventional wells.

streams were monitored by the facility. Two of the streams (m- and z-) occur outside the plume footprint and therefore are not considered further. Smaller tributaries originate in wetland areas along the lower terrace, feeding into x- and y-streams which converge prior to discharging directly to the river.

3. Field and laboratory methods

This study was conducted in July and October 1999 (Phase 1) and August and December 2000 (Phase 2). The VOC distribution was determined in detail in the groundwater zone using depth-

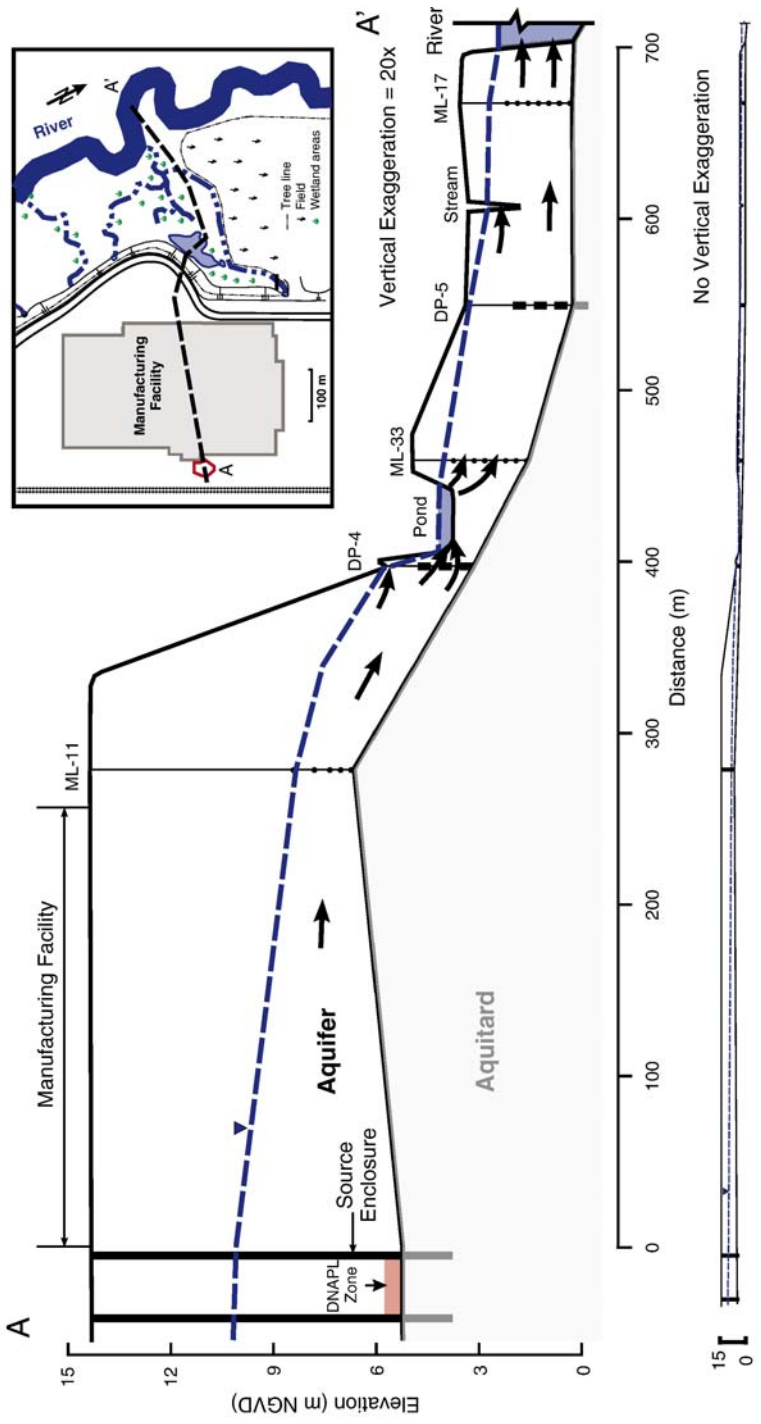

Fig. 2. Longitudinal cross-section from the facility to the river (the inset shows details on surface cover, vegetation, wetland areas, etc.).

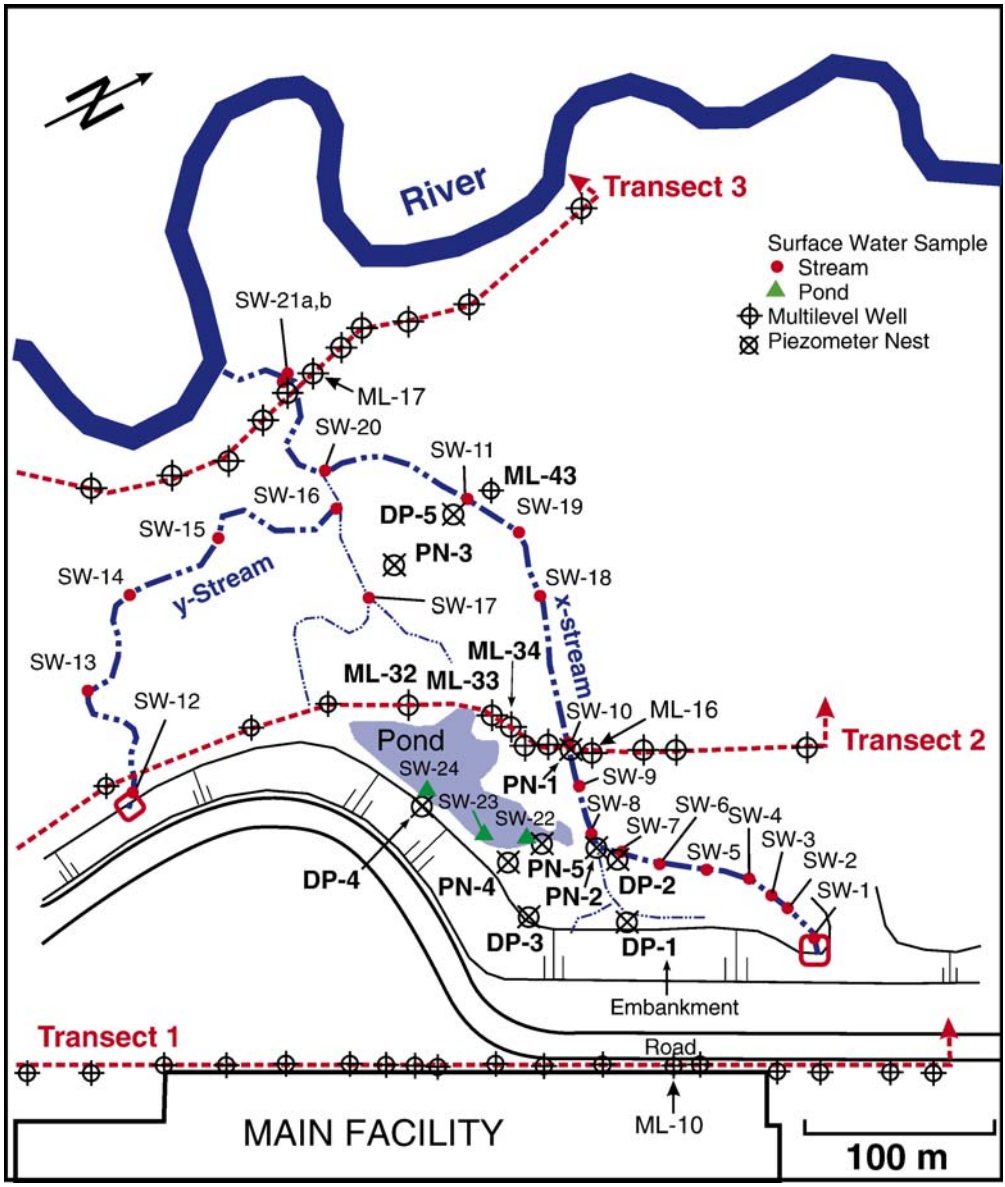

Fig. 3. Plan view blowup of the area between Transect 1 and the river showing locations of monitoring transects, piezometer nests, surface water features (pond, streams, river) and surface water sampling locations.

discrete sampling techniques (Waterloo Profiler, multilevel samplers, piezometer nests) and in surface water bodies (streams and pond) along the plume flowpath. Sampling was also conducted to investigate aquifer hydrogeochemical conditions at selected locations to determine the potential for degradation, and compound-specific carbon isotopes were applied as a tool for assessing degradation in the groundwater zone.

3.1. Groundwater sampling

Plumes emanating from DNAPL source zones typically exhibit significant internal concentration variability (e.g. Cherry, 1997; Cherry and Parker, 1997; Guilbeault et al., 2005). Thus collection of data to clearly demonstrate the magnitude of and processes causing plume attenuation is not an easy task. A method gaining acceptance is the transect approach (e.g. Barker et al., 2000; Einarson and Mackay, 2001; Guilbeault et al., 2005), which involves application of depth-discrete monitoring along cross-sections (i.e. transects) across the plume at different distances along its flowpath. Monitoring may be conducted using multilevel samplers (e.g. Cherry et al., 1983; Einarson and Cherry, 2002) or the Waterloo Profiler (Pitkin et al., 1999) to provide high resolution of the contaminant distribution within the plume. Contaminant mass discharge estimates across the transects can be made using the contaminant distribution along with measured or estimated Darcy flux, and reductions in mass discharge between transects can be used to provide direct evidence of plume attenuation.

In this study, the contaminant distribution in the aquifer was determined by groundwater monitoring along three transects perpendicular to groundwater flow (Fig. 1): Transect 1 along the upper terrace just west of the building 280 m from the source, Transect 2 along the lower terrace midway between the building and river with a portion of the transect just downgradient of the pond, and Transect 3 along the edge of the river 700 m from the source. Two complete transect sampling episodes were conducted: July 1999 (Phase 1) and August 2000 (Phase 2). Transect monitoring was conducted using multilevel samplers and the Waterloo Profiler; multilevels were used entirely for Transect 1 while both were used for Transects 2 and 3. Rapid on-site VOC analyses allowed sampling decisions to be made in the field. During Phase 2, several Profiler locations were replaced with multilevels and additional locations were investigated. In total, 46 locations were investigated using multilevels and 22 using the Profiler, with a total of 57 unique locations along the three transects.

Multilevels were of the type described by Cherry et al. (1983). Each multilevel had between 4 to 8 sampling points, consisting of 1.3 cm OD polyethylene tubes with 10 cm long intakes wrapped with Nitex™ fabric, bundled around a 1.9 cm OD Schedule 80 PVC pipe, with the bottom 15 cm screened to serve as the bottommost sampling point. Cores were collected at each location using the piston coring system described by Zapico et al. (1987) and Enviro-Core direct push driving of casing (Einarson, 1995; Einarson et al., 1998) to accurately determine the depth to the top of the aquitard. Multilevels were constructed with the bottom sampling point positioned at the base of the aquifer and top point close to the water table. Vertical spacing of intermediate points ranged from 0.3 to 1.0 m, with tighter spacing near the bottom of the aquifer. Multilevels were installed through 8.9 cm OD casing, driven to the target depth with an aluminum knock-out plug using a truck-mounted Enviro-Core rig. Following insertion of the multilevel, the casing was withdrawn and aquifer sand collapsed around the multilevel, except above the water table where bentonite was placed to ground surface. Groundwater samples were collected using a peristaltic pump and dedicated 6.4 mm OD Teflon™ sample tubes for each multilevel, which was inserted into the polyethylene tubes into the screened intake. After purging at least two tubing volumes, the pump was shut off (maintaining the vacuum at surface), the sample tube withdrawn from the multilevel point, with the outside dried using a clean paper towel during removal, the pump reversed or suction released and groundwater in the sample tube pumped or drained into a 25 mL glass vial, filling into the bottom of the sample bottle and allowing overflow before capping to minimize sample contact with air. This method minimizes potential for bias due to volatile loss, and avoids use of a sampling head at surface or requirement for decontamination of the pump tubing. It also avoids contact of the groundwater sample with the polyethylene tubing used for the

multilevel points, and thus potential for cross-contamination via diffusion through the tubing. The Teflon™ sample tube was decontaminated between points by flushing with methanol and distilled water. Samples were also collected from the top to bottom point on each multilevel (lowest to highest concentrations) to minimize carryover effects.

The Waterloo Profiler (Pitkin et al., 1999), a direct-push tool for collecting depth-discrete groundwater samples in unconsolidated granular deposits, was used along Transects 2 and 3 where the water table was shallow (<3 m). The Profiler was advanced using a track-mounted Enviro-Core rig. Vertical sample spacing ranged from 0.15 to 0.6 m. The aquitard depth was determined from monitoring pressure and rate of distilled water injection, which is done while advancing the Profiler tip between sample depths (to avoid clogging of the sampling ports), and a minimum of 200 mL was purged prior to sample collection to remove distilled water from the stainless steel tubing and ensure the sample was from the aquifer. Most Profiler locations were completed in less than two hours.

Locations inaccessible to drilling equipment (between transects and beneath stream beds) were investigated using piezometer nests (Fig. 3). The DP-series piezometers consist of stainless steel drive-points with 15 cm long screens coupled to 1.9 cm OD steel pipe, with 1.3 cm OD polyethylene tubing connected to the top of the piezometer tip, running inside the steel pipe to surface for water level measurements and sampling. These were manually driven using a drive-head and sledge hammer. Each DP-series nest had three to four piezometers installed to depths ranging from 0.6 to 3.6 m bgs. The PN-series piezometers consist of 1.3 cm OD polyethylene tubes with 10 cm Nitex™ wrapped intakes, installed using 2.5 cm OD steel pipe driven manually to the target depth with a knock-out plug, which was then retracted leaving the piezometer in place. The PN-series nests each had between three to five piezometers installed to depths ranging from 0.6 to 2.6 m bgs. Samples were collected from piezometers using a peristaltic pump and dedicated 6.3 mm OD Teflon™ tubing.

3.2. Surface water sampling

Surface water samples for VOC analysis were collected from the pond, streams and seeps near the base of the embankment in August 2000, at the same time as the Phase 2 sampling of transects for groundwater analysis. Pond samples were collected at three locations (Fig. 3) along the upgradient side close to the bottom (within ~10 cm), and two locations were re-sampled in December 2000 when the pond surface was frozen. Samples were collected along x- and y-streams at 21 locations (Fig. 3) from the outfalls to Transect 3, from near the bottom of the streams (within ~10 cm) where possible. Surface seepage samples were collected along the base of the embankment near several piezometer nests (DP-1, DP-3, DP-4, PN-4; Fig. 3) by excavating a shallow hole and collecting a grab sample as it filled with water.

3.3. Groundwater VOC analyses

The July 1999 and August 2000 samples were analyzed for VOCs on-site in a mobile lab using a SRI 8610C portable gas chromatograph (GC) equipped with photo ionization (PID) and flame ionization (FID) detectors, using a solid-phase microextraction (SPME) headspace technique (Pawliszyn, 1997; Górecki and Pawliszyn, 1997). Concentrations were quantified using calibration curves generated daily from eight standards and lab blanks. Duplicates and standard checks were routinely analyzed. Method detection limits (MDLs) for Phase 1 were 10 μg/L for TCE, PCE and the DCE isomers and 90 μg/L for VC; the method was improved for Phase 2 with lower MDLs of 1 μg/L for TCE, PCE and the DCE isomers and 50 μg/L for VC. Rapid sample

turnaround times allowed field modifications to the sampling program, which was particularly useful during Phase 1 in conjunction with sampling using the Waterloo Profiler.

The December 2000 samples were analyzed for VOCs in a fixed lab by liquid–liquid extraction using pentane (capillary GC grade). Two milliliter of water sample were extracted with 2 mL of pentane on an orbital shaker for 15 min, followed by direct injection of 1 μL of pentane extract on a HP 6890 GC (in splitless mode at 225 °C and 3 mL/min helium carrier gas flow) equipped with a liquid auto sampler, an HP 624 column (30 m long, 0.32 mm ID, 1.8 μm film thickness) and an electron capture detector (ECD). The temperature program was 4 min at 35 °C, ramping to 60 °C at 10 °C per min and then to 105 °C at 30 °C per min and held for 2.5 min. Concentrations were quantified using calibration curves generated from seven standards, prepared by injecting methanolic stock solutions into water and then extracting with pentane using the same pentane to water ratio and extraction time used for the samples. Dilutions of samples into deionized water were performed if required based on initial analysis of the undiluted sample. Duplicates, lab blanks and standard checks were routinely analyzed. MDLs were 1 μg/L for TCE and PCE and 100 μg/L for the DCE isomers; VC was not quantified.

3.4. Hydrogeochemical evaluation

Hydrogeochemical sampling was conducted at selected locations along the plume flowpath in October 1999 (Phase 1) to assess the potential for reductive dechlorination: ML-10 (Transect 1), DP-2 (between Transects 1 and 2), ML-16 (Transect 2), DP-5 (between Transects 2 and 3) and ML-17 (Transect 3). Field measurements of pH, redox potential and conductivity were performed using electrodes and flow-through cells downstream of a peristaltic pump. Alkalinity was measured using a HACH™ test kit. Dissolved oxygen (DO) was measured using CHEMetrics™ test kits (0–2 mg/L range, detection limit 0.05 mg/L; 0–15 mg/L range, detection limit 0.4 mg/L) and a VVR multi-analyte photometer, with samples collected by slowly pumping into a 125 mL flask allowing overflow at the top and using self-filling ampoules. For silty samples where positive bias may occur, samples were filtered (0.45 μm syringe filters) and tests were repeated, which generally provided lower DO values; however exposure to air during filtering may also bias results such that lower end results (0.5 to 1 mg/L range) may represent anaerobic conditions. Samples for inorganic parameters were collected in two 60 mL plastic bottles, with the cation sample field filtered and acidified, and shipped to PSC Analytical Services in Halifax, Nova Scotia for analysis of parameters in the RCAp-30 package (including chloride, nitrate, sulfate, iron and manganese). Samples for analysis of dissolved hydrocarbons (methane, ethane and ethene) and total and dissolved organic carbon (TOC/DOC) were collected in 25 mL glass vials and submitted to the University of Waterloo Organic Geochemistry Lab for analysis using a GC headspace equilibration technique (Kampbell et al., 1989) and Dohrmann DC190 carbon analyzer, respectively.

3.5. Compound specific carbon isotopes

Compound-specific carbon isotopes are a promising tool for investigating biodegradation of chlorinated solvents (e.g. Meckenstock et al., 2004). Lab studies (Hunkeler et al., 1999; Sherwood Lollar et al., 1999; Bloom et al., 2000; Slater et al., 2001) show appreciable fractionation (enrichment in ^{13}C) during microbial reductive dechlorination of TCE (i.e. TCE → *cis*-DCE → VC → Ethene). Similar shifts have also been observed at field sites where dechlorination is occurring (Hunkeler et al., 1999; Sherwood Lollar et al., 2001). Of particular interest is the large fractionation associated with the final two dechlorination steps, which can provide strong evidence

that complete dechlorination is occurring. Lab studies (Dempster et al., 1997; Harrington et al., 1999; Huang et al., 1999; Slater et al., 1999, 2000) have shown minimal isotope fractionation occurs under non-degradative processes such as sorption, dissolution and volatilization. Field studies at two sites (Hunkeler et al., 2004) showed that PCE and TCE isotope ratios were stable along plume flow paths where little or no degradation was occurring.

In this study, 54 samples were collected for isotope analyses (December 2000) from selected multilevels: Transect 1: ML-10, ML-11 and ML-26; Transect 2: ML-16, ML-18, ML-32 and ML-34; and Transect 3: ML-40 and ML-42; from piezometer nests DP-1, DP-4, DP-5, PN-3 and PN-4 and from the pond. Analyses were performed using methods described by Hunkeler et al. (2004), which allow determination on samples with very low (μg/L range) VOC concentrations. Duplicate samples were collected from each location for VOC analyses as described earlier. Results of TCE isotope analyses on groundwater and DNAPL samples from the source zone (Hunkeler et al., 2003) provide the starting composition for comparison to plume results. Carbon isotope data are reported using delta notation; defined as $\delta^{13}C = (R_s/R_r - 1) \times 1000$, where R_s and R_r are the $^{13}C/^{12}C$ ratios of the sample and a reference standard, respectively.

4. Results and discussion

4.1. VOC distribution and mass discharge across the transects

The distribution of VOCs along the transects and estimates of mass discharges are first presented, showing the plume is strongly attenuated in the groundwater system. Causes of attenuation are then evaluated focusing on the effects of groundwater–surface water interactions with the pond and streams and evidence for degradation. Water table contours from measurements in several conventional monitoring wells (September 1999) show the three transects are well-positioned to monitor the plume downgradient of the DNAPL source (Fig. 1). Distributions of TCE and *cis*-DCE along the transects from Phase 2 (August 2000) are provided in Figs. 4 and 5, respectively. Phase 1 (July 1999) results, not included here, were similar. The TCE plume along Transect 1 (Fig. 4a) just west of the building was > 300 m wide, with the highest concentrations at the base of the aquifer and declining considerably within a few 10s of cm above the interface. The plume width, much wider than the isolated DNAPL source zone, is attributed to divergence of groundwater flow lines (evident in Fig. 1) and minor effects of transverse horizontal dispersion (Chapman and Parker, 2005). Maximum TCE concentrations (at ML-15) were 34,000 and 25,500 μg/L in 1999 and 2000, respectively. In comparison, *cis*-DCE was only sporadically detected (Fig. 5a), and at much lower concentrations than TCE, while VC was not detected. The occurrence of only minimal TCE degradation products along with the isotope results (described later) suggests minimal transformation over the 280 m distance between the source and Transect 1.

The TCE plume along Transect 2 (Fig. 4b) had a similar width as Transect 1 but much lower concentrations, with maximums of 3100 and 2400 μg/L in 1999 and 2000, respectively. The highest values (at ML-18) occur where Transect 2 intersects x-stream, while much lower concentrations were observed downgradient of the pond. Results from piezometer nests upgradient of the pond are presented later for comparison and evaluation of pond effects. The distribution of *cis*-DCE (Fig. 5b) generally overlaps with TCE, with a maximum concentration of 500 μg/L and exceeding TCE in many points. VC was not detected along Transect 2, although the relatively high MDLs may mask some occurrence since VC was detected in piezometer nests upgradient of Transect 2 (examined later). Transformation of TCE to *cis*-DCE between Transects 1 and 2 is consistent with hydrogeochemical conditions and carbon isotope results described later. Along Transect 3 near

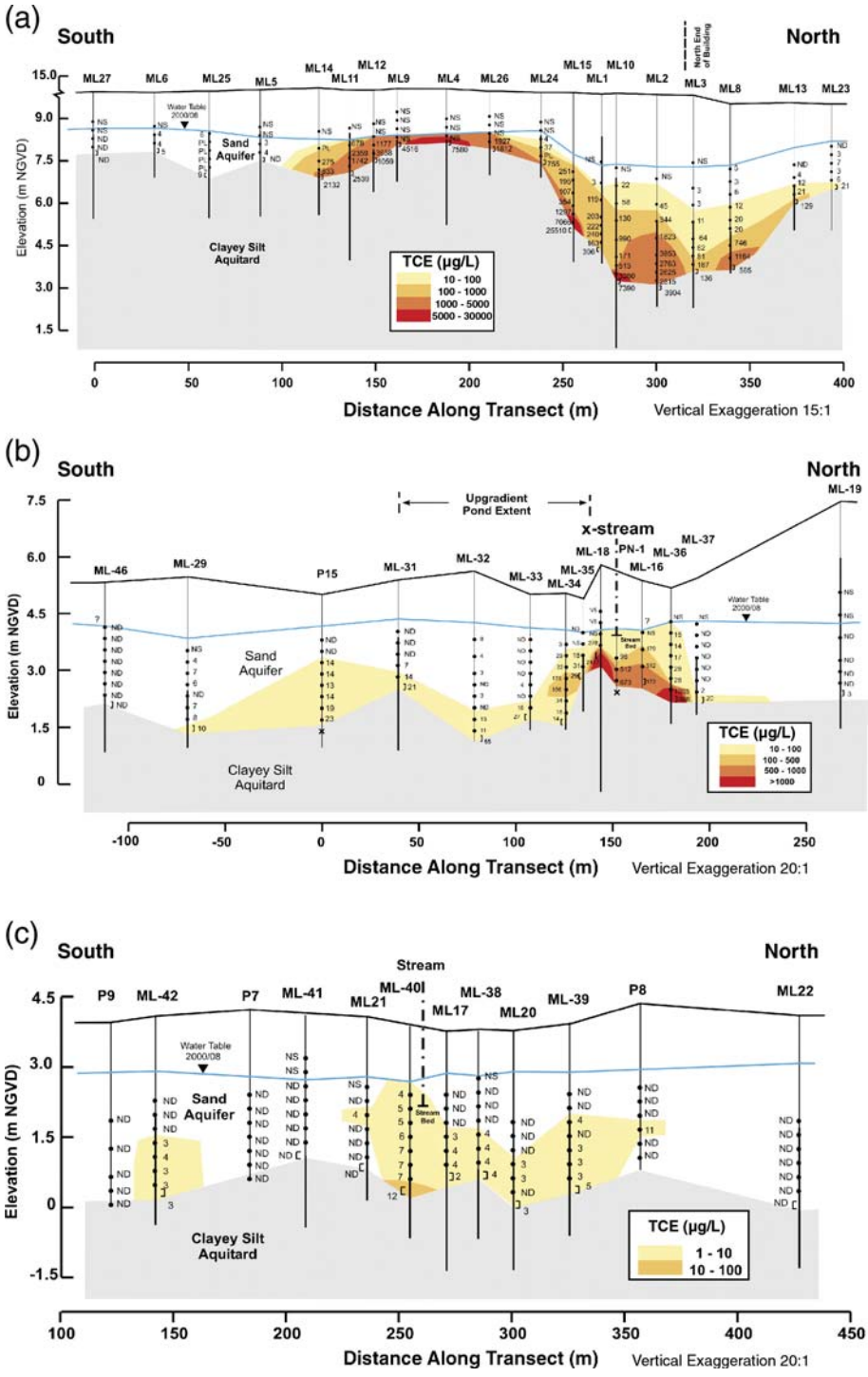

Fig. 4. Contours of TCE along (a) Transect 1, (b) Transect 2 and (c) Transect 3 from August 2000.

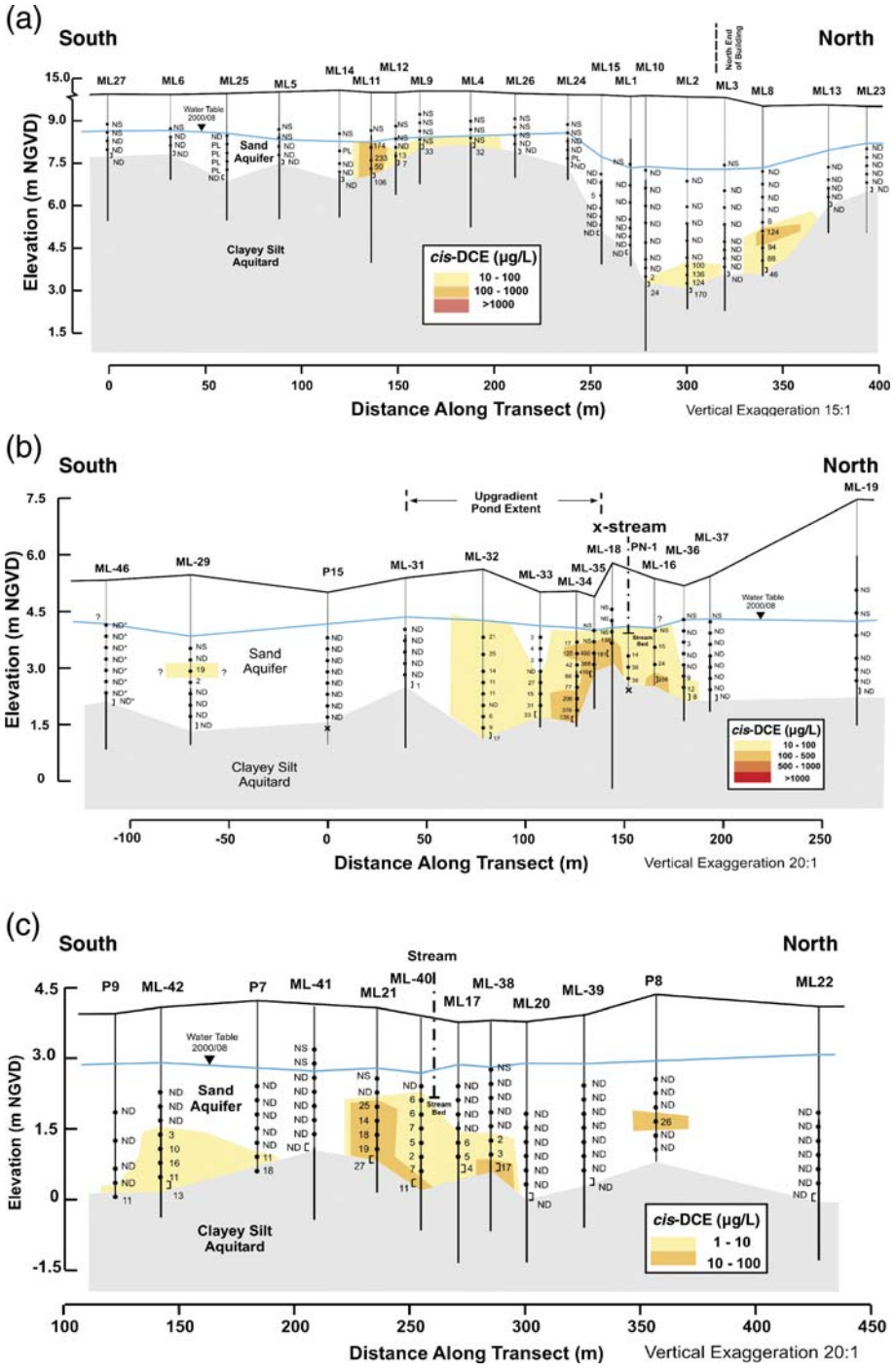

Fig. 5. Contours of *cis*-DCE along (a) Transect 1, (b) Transect 2 and (c) Transect 3 from August 2000.

the edge of the river, both TCE (Fig. 4c) and *cis*-DCE (Fig. 5c) concentrations were very low (<30 µg/L). The distribution of *cis*-DCE again overlaps with TCE, with *cis*-DCE exceeding TCE in most points where both were detected. VC was not detected along Transect 3.

The detailed transect monitoring shows maximum TCE concentrations in groundwater decline by more than three orders of magnitude along the plume flowpath between Transects 1 to 3 with negligible accumulation of degradation products (Fig. 6a). Therefore, based on groundwater

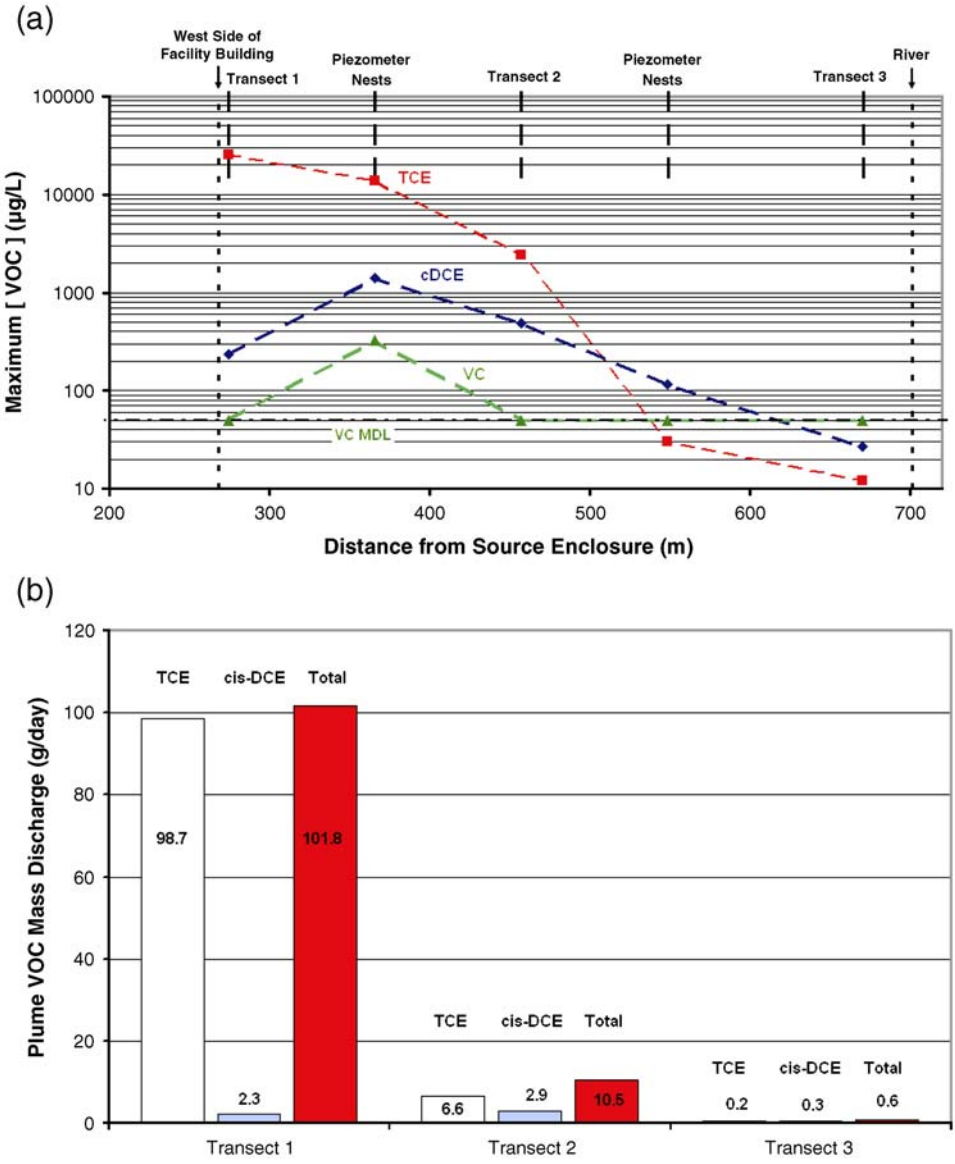

Fig. 6. Plots showing (a) maximum VOC concentrations observed along the three main transects and in piezometer nests located between the transects; and (b) estimated VOC mass discharge across the transects (TCE, *cis*-DCE and total (as TCE)).

concentration data, the TCE plume appears to be strongly attenuated between the facility and river. To better quantify plume attenuation, and for later comparison with stream mass discharge, VOC mass discharges across each transect were estimated using the approach described by Einarson and Mackay (2001) and Guilbeault et al. (2005) by:

$$M_d = \sum_{i=1}^{n} C_i A_i q_i \tag{1}$$

where M_d is the total contaminant mass discharge (mass/time), C_i is the concentration (mass/volume) assigned to transect area element A_i (area) with Darcy Flux q_i (volume/area/time). In this case, C_i is the VOC concentration at each monitoring point applied over A_i, approximated as a rectangle with a width of half the distance to adjacent multilevels and a height of half the vertical interval between sampling points above and below, except for the bottommost point at the interface where only the upper half-distance was applied. A groundwater specific discharge (i.e. Darcy Flux) (q_i) of 0.21 m/day was estimated using Darcy's Law ($q = K\,i$) applying the geometric mean aquifer hydraulic conductivity (K) from slug tests by consultants in 37 conventional wells across the site (1.5 to 3.0 m long screens) of 2.4×10^{-4} m/s and average hydraulic gradient (i) of 0.01 (Fig. 1). Relative to the hydraulic conductivity of this nearly homogeneous aquifer and differences in the hydraulic gradient along the transects, spatial variability in VOC concentrations is large, therefore the Darcy flux value was uniformly applied along the transects. Applying an aquifer porosity (ϕ) of 0.35, the average linear groundwater velocity ($\overline{v} = q/\phi$) is 0.6 m/day, consistent with results of *in situ* borehole dilution tests (Chapman and Parker, 2005) performed at two locations along the lower terrace and 3 to 4 depths at each location, which provided a groundwater velocity range of 0.2 to 1.4 m/day and average of 0.7 m/day. The average groundwater velocity estimate is further supported by the lag time for declines in groundwater TCE concentrations in monitoring wells just downgradient of Transect 1 following source zone isolation (Chapman and Parker, 2005).

Mass discharges were estimated separately for TCE and *cis*-DCE and the total discharge (as TCE) was calculated by:

$$TCE_{total} = TCE + 1.35\ cis DCE \tag{2}$$

which accounts for the *cis*-DCE mass being derived from TCE degradation. Similar to peak concentrations, VOC mass discharge in the groundwater system also declines significantly along the plume flowpath (Fig. 6b) with the total mass discharge declining from more than 100 g/day across Transect 1 to about 10 g/day across Transect 2 and < 1 g/day across Transect 3. These mass discharge estimates confirm the strong groundwater plume attenuation apparent from detailed concentration data. The groundwater travel time from the source zone to the river (~ 700 m) was about 3 years based on the average groundwater velocity estimates; therefore the plume advective front would have flushed through the system decades ago and the strong attenuation observed is not related to monitoring beyond the advective front. The small mass discharge crossing Transect 3 shows that direct input of VOC mass from groundwater discharge to the river is small. The total groundwater discharges (sum of the Darcy flux q_i in equation 1) were 161,000, 169,000 and 122,000 L/day (transect areas of 777, 816 and 591 m^2) across the entire areas of Transects 1, 2 and 3, respectively; however, discharges in the zone actually occupied by the VOC plume were lower. This suggests a small increase in groundwater flow (net recharge to groundwater) between Transects 1 and 2 and a loss (net discharge from groundwater) to surface water between Transects 2

and 3. The plume mass discharge estimates at the transects do not account for groundwater discharge to surface water upgradient of the river, and therefore partial plume mass discharge that may be occurring to the streams between Transects 1 and 3. Stream VOC mass discharges are examined later for comparison to groundwater mass discharge.

4.2. Plume discharge to pond

The pond intercepts roughly the southern half of the plume along the lower terrace upgradient of Transect 2 (Figs. 3, 4b and 5b). The conceptual model for the shallow pond, which has no surface inflows or outflows, has groundwater discharging near the upgradient side, flowing through the pond, and then recharging back to the groundwater system near the downgradient side. Geometry of the aquifer and pond and comparison with scenarios in Townley and Davidson (1988) suggest the pond capture zone in plan view is likely slightly larger than the length perpendicular to groundwater flow (>100 m), consistent with water table contours in the pond vicinity (Fig. 1). In vertical section, the pond is expected to capture nearly all groundwater flow with minimal bypass (underflow), since the aquifer thickness in the area of the pond (1–3 m) is much smaller than the pond width parallel to groundwater flow (~30 m). Groundwater discharge to the pond is expected to occur within a short distance from the upgradient side, passing through the pond, and then recharging back to the groundwater system within a short distance of the downgradient side. Comparison of the surface water elevation in the pond to the hydraulic head in a piezometer installed below the pond bottom near the downgradient side shows a strong downward gradient (~0.2) supporting this interpretation. Cross-sectional modeling of the groundwater system in the area of the pond (results not provided here) further supports minimal to no pond underflow. VOC results (August 2000) from three locations along the upgradient side of the pond (Fig. 3) confirms significant plume discharge, with the highest VOC concentrations at the northern end (SW-22: TCE=1400, *cis*-DCE=2400, VC=60 μg/L), lower concentrations at the middle location (SW-23: TCE=350, *cis*-DCE=200 μg/L) and lowest at the southern end (SW-24: TCE=100, *cis*-DCE=20 μg/L).

Comparison of groundwater VOC concentration profiles from piezometer nests upgradient (Fig. 7a) and multilevels downgradient (Fig. 7b) of the pond clearly show the effects of the pond. The highest upgradient TCE concentrations occurred at PN-4 (>13,000 μg/L) near where the highest pond concentrations were observed. Shallower points showed lower TCE concentrations, but elevated levels of degradation products *cis*-DCE and VC (including the maximum VC concentration of 330 μg/L observed during this study), supporting occurrence of degradation within the aquifer before discharging to the pond. Lower concentrations were observed at DP-4 (maximum TCE was 550 μg/L) which is consistent with lower pond concentrations in this area. TCE profiles were similar in December 2000 at both nests, with slightly lower concentrations in deeper points and higher concentrations in shallower points. In contrast, multilevels most directly downgradient of the pond (ML-32, ML-33) showed much lower TCE and *cis*-DCE concentrations in August 2000 (<30 μg/L) with *cis*-DCE exceeding TCE in most points. Higher concentrations were observed at ML-34 (<400 μg/L), presumably due to lower pond width and higher upgradient concentrations in this area.

The strong decline in VOC concentrations in groundwater up-and down-gradient of the pond is attributed to: (1) dilution, (2) VOC mass escape across the pond surface to the atmosphere, and (3) degradation during discharge and recharge through pond bottom sediments. Dilution in the pond occurs due to mixing of plume groundwater at different concentrations with uncontaminated groundwater discharged to the pond and precipitation. Preliminary evaluation of VOC mass loss

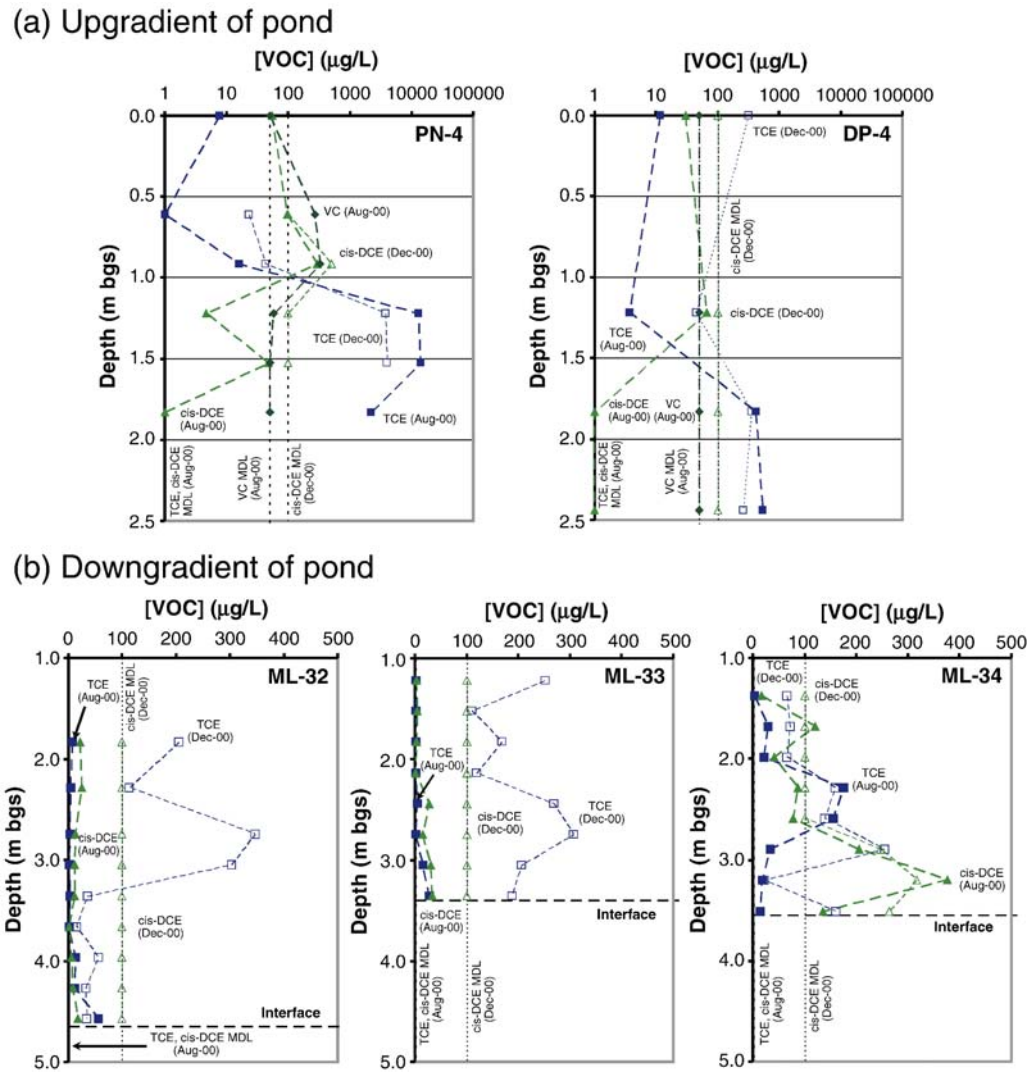

Fig. 7. Profiles of TCE (squares), *cis*-DCE (triangles) and VC (diamonds) in (a) piezometer nests DP-4 and PN-4 upgradient of the pond; and (b) multilevels ML-32, ML-33 and ML-34 downgradient of the pond. Results are shown for August (solid symbols) and December 2000 (hollow symbols). VC was not analyzed in December samples. Concentrations plotted at the zero depth represent near surface samples collected as described in the text.

due to water–air exchange from the pond was performed using box-model calculations described by Schwarzenbach et al. (2003), where VOC mass transfer is governed by groundwater input/output, residence times, pond depth, volume and surface area, vertical mixing, wind speed, water temperature and Henry's coefficient. Simplified calculations using estimated site parameters provided a first-order rate constant for water–air exchange of 0.8 day^{-1}. Pond residence times are estimated to be several days to a few weeks; therefore, based on this calculation, much of the decline in VOC concentrations, from 1000s of µg/L at the upgradient side of the pond to 10s of µg/L downgradient, can be attributed to mass transfer to the atmosphere. Assumptions inherent in

such calculations (e.g. well-mixed conditions vertically in the pond) provide uncertainty and may lead to overestimation of mass loss via volatilization. Degradation may also be significant during discharge to the pond and recharge back to the groundwater system, with the likely presence of organic rich pond-bottom sediments. Detailed investigation of the pond bottom was not carried out; however, other studies have shown significant degradation of chlorinated VOCs near groundwater–surface water interfaces (e.g. Lorah and Olsen, 1999; Conant et al., 2004). Carbon isotope data discussed below provides evidence for TCE degradation during groundwater discharge into the pond. However, the relative contribution of volatilization versus degradation to the strong VOC concentration decline across the pond at this site would be difficult to ascertain without more detailed study.

The pond also causes large seasonal variation in VOC concentrations downgradient in the groundwater. Longer-term monitoring of two conventional wells immediately downgradient of the pond (MW-03, MW-04; Fig. 1) conducted quarterly from 1991–1995 (Mar, Jun, Sept, Dec) and semi-annually from 1996–2000 (Mar, Sept) by consultants showed large (order of magnitude or greater) variation in VOC concentrations, with highest concentrations consistently observed in March sampling events and lowest in September. During this study, higher pond VOC concentrations were observed near the upgradient side in December 2000 samples collected below the frozen surface (SW-22: TCE=1800, *cis*-DCE=440 μg/L; SW-23: TCE=3040, *cis*-DCE=1540 μg/L) compared to August results (particularly at SW-23). Increase in pond VOC concentrations was also reflected in downgradient multilevels in the December samples, with TCE increasing to 300–350 μg/L at ML-32 and ML-33 (Fig. 7b). Based on the conventional well results, concentrations likely become even higher later in the winter as the pond surface is frozen for a longer period of time. While much of this increase was likely due to limited escape of mass from the pond to the atmosphere due to frozen surface conditions, degradation rates may also decline in the winter due to lower microbial activity at lower temperatures.

4.3. Groundwater seeps at base of embankment

Groundwater seeps were evident at locations near the base of the embankment, which would allow VOC mass loss from the groundwater system due to water–air exchange. Discharge was most evident in the area of piezometer nests DP-1 and DP-3 (Fig. 3) with VOC results plotted at zero depth in Fig. 8. The relatively high VOC concentrations in near-surface groundwater samples at DP-1 (July 1999: TCE=40, *cis*-DCE=230, VC=100 μg/L; August 2000: TCE=110, *cis*-DCE=25 μg/L) and DP-3 (July 1999: TCE=1970, *cis*-DCE=85 μg/L; August 2000: TCE=340, *cis*-DCE=20 μg/L) confirm plume discharge to surface via seeps. Upgradient of the pond, VOC concentrations in near-surface samples were lower at DP-4 (TCE=12, *cis*-DCE=30 μg/L) and PN-4 (TCE=8, *cis*-DCE=54 μg/L) in August 2000. While VOC mass loss to the atmosphere due to groundwater seepage is difficult to quantify, it may be another mechanism contributing to apparent plume attenuation. Occurrence of TCE degradation products also suggest TCE transformation is enhanced but not complete during passage through organic-rich sediments prior to discharge, which is confirmed by the carbon isotope data discussed below.

4.4. Plume discharge to streams

Discharge of the plume to streams along the lower terrace, with subsequent mass transfer from the streams to the atmosphere (Rathbun, 1998; Schwarzenbach et al., 2003) also appears to

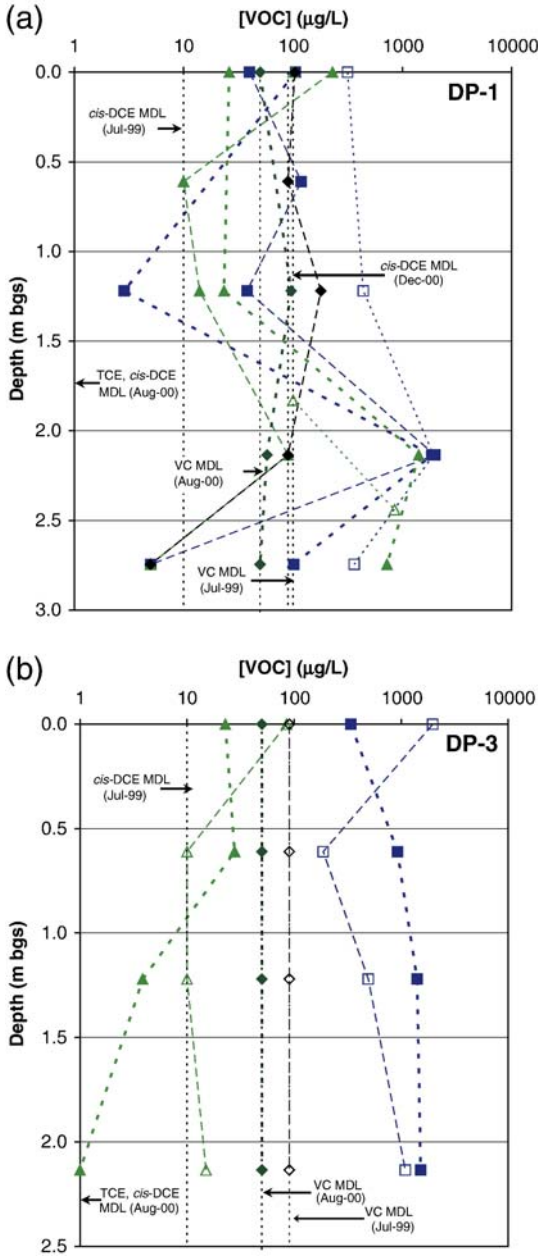

Fig. 8. Profiles of TCE (squares), *cis*-DCE (triangles) and VC (diamonds) in piezometer nests near the base of the embankment: (a) DP-1 and (b) DP-3 from Phase 1 field episode in July 1999 (solid symbols, long dash) and Phase 2 field episodes in August (solid symbols, short dash) and December 2000 (hollow symbols). VC was not analyzed in December samples.

contribute to apparent plume attenuation. Woessner (2000) examines conceptual scenarios of groundwater–stream interactions which are used in the discussion below. VOC concentrations in samples collected along x-and y-streams (SW-1 to SW-21; Fig. 3) provide evidence for plume

discharge. Where VOCs were detected, TCE generally exceeded *cis*-DCE, and VC was not detected in any stream samples. At the outfalls where x- and y-streams begin (SW-1, SW-12) VOCs were not detected, indicating downstream occurrences result from plume discharge. Along the initial stretch of x-stream perpendicular to groundwater flow (SW-2 to SW-7) TCE concentrations increased from non-detect to 8–10 μg/L, likely a 'flow-through' reach where shallow groundwater discharges to the stream along the upgradient side and mixed groundwater/surface water recharges along the downgradient side. At the stream bend, piezometer nest PN-2 (Fig. 3) showed TCE concentrations of 40, 70 and 1260 μg/L at 1.0, 1.5 and 2.0 m below the stream bed. After the bend, x-stream flows over a small spillway (~0.3 m high) which likely enhances VOC loss to the atmosphere. Stream TCE concentrations increased from 10 μg/L after the spillway (SW-8) to 34 μg/L (SW-9) to 60 μg/L at Transect 2 (SW-10). The piezometer nest along Transect 2 (PN-1) showed TCE concentrations of 100, 510 and 670 μg/L at 0.6, 0.9 and 1.2 m below the stream bed (Fig. 4b). The abrupt drop in stream level at the spillway likely causes greater groundwater discharge to the stream along this stretch (i.e. a 'gaining' reach).

The plume distribution along Transect 2 (Figs. 4b and 5b) shows the highest concentrations occur in the vicinity of x-stream, indicating its potential for strong influence on the plume. Water table contours (Fig. 1) also show x-stream has a strong hydraulic influence on groundwater flow, suggesting the stream is gaining between Transects 2 and 3, further supported by transect groundwater flow estimates. Between Transect 2 and before the convergence with y-stream (SW-18, 19, 11), x-stream TCE concentrations remained relatively steady (40–50 μg/L) and similar to that observed at Transect 2 (SW-10), suggesting that VOC increases in the stream due to plume discharge may be offset by mass loss from the stream to the atmosphere. TCE concentrations along y-stream are very low (<1 to 3 μg/L) before it converges with x-stream (SW-13 to SW-16) indicating only small plume discharge to this (y-) stream. A small tributary originating in a wetland area (SW-17) also had no detectable VOCs. Where x- and y-streams converge (SW-20) dilution caused lower TCE concentration (30 μg/L) than observed upstream (in x-) although stream contents would not be well-mixed at this point. At Transect 3 just prior to discharging to the river, TCE concentrations were 70 and 20 μg/L in samples collected from the north (SW-21a) and south (SW-21b) banks of x-stream, respectively. Surface water samples were not collected from the river during this study; however results of regular river sampling ~20 m downriver of the stream discharge point by consultants show concentrations consistently below MDLs. The combined x- and y-stream flows at the time of sampling (795,000 L/day, see below) and average annual river flow (7.3×10^8 L/day) provides a dilution factor of 920, therefore the reduction from 10s of μg/L in the stream to below MDLs in the river is expected.

Stream mass discharges were calculated at transect intersections for comparison to groundwater plume mass discharges, by multiplying stream concentrations and estimated stream flow rates. Stream flow rates were taken as the stream inputs monitored by the facility on the day of sample collection (in August 2000), assuming changes in stream flow due to groundwater interactions are minor. This assumption can be justified by comparing the stream volumetric input from the facility at the outfall (stream starting point) with potential groundwater discharge; for example, assuming all groundwater within a zone ~20 m on either side of x-stream along Transect 2 (between ML-34 and ML-36) discharges directly to the stream, this groundwater input would represent less than 5% of the input to x-stream at the outfall. TCE concentrations were also assumed to be uniform within the stream channel for the stream mass discharge estimates. Where x-stream crosses Transect 2, the TCE mass discharge in the stream (flow rate of 568,000 L/day, TCE concentration of 60 μg/L) was 34 g/day, five times higher than the subsurface plume mass

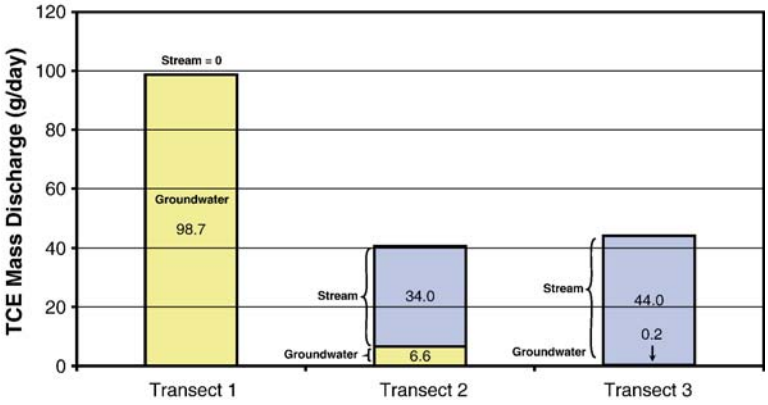

Fig. 9. Plot comparing estimated TCE mass discharge in the plume and in the stream where it crosses Transects 2 and 3.

discharge across Transect 2 (Fig. 9). The stream channel at this location was about 1.8 m wide and 0.3 m deep; dividing the flow rate by the cross-sectional area gives an average stream velocity of 1050 m/day, indicating a 0.2 day travel time to the river. Where the combined x-and y-streams cross Transect 3, the stream channel was about 3.0 m wide and 0.7 m deep with more sluggish flow. Multiplying the combined stream inputs (795,000 L/day) with a weighted TCE concentration of 55 μg/L (based on relative inputs from each stream, assuming the x-stream flow applies to the sample from the north bank and y-stream flow to that from the south bank), provides a stream TCE mass discharge of 44 g/day, more than two orders of magnitude higher than the Transect 3 plume mass discharge (Fig. 9). The total stream discharge to the river (795,000 L/day) is a factor of 6.5 higher than the estimated groundwater discharge across Transect 3 (122,000 L/day). The stream TCE discharge estimates show that nearly 50% of the plume discharge across Transect 1 reaches the river directly via streamflow. It is likely that even more of the plume mass discharge is lost to the streams than estimated based on stream concentrations and volumetric discharge, due to mass loss from the stream to the atmosphere via volatilization prior to discharging to the river, which was not measured in this study.

4.5. Evidence for VOC degradation

The distribution of VOCs along the transects (Figs. 4 and 5) and scatter plots showing TCE versus *cis*-DCE for each transect (Fig. 10) show minimal degradation between the source zone and Transect 1, but much greater TCE transformation to *cis*-DCE further downgradient along the lower terrace. VC was only observed in a few piezometers near the base of the embankment and not along the transects. Although detections of VC could be masked by the elevated MDLs (50–90 μg/L), VC mass appears to be negligible. Groundwater monitoring clearly shows that TCE disappears from the groundwater system, but that TCE degradation products (*cis*-DCE, VC) do not accumulate significantly within the plume (Fig. 6a). One explanation is that TCE transformation stalls at *cis*-DCE and the mass loss from the groundwater system is due almost entirely to seeps and discharges to surface water (pond and streams), and subsequently by volatilization and direct discharge to the river via the streams. Alternatively, complete dechlorination to non-chlorinated end products (e.g. ethene) may cause substantial loss of VOC mass. The lack of VC may be a result of reductive dechlorination or direct aerobic or anaerobic oxidation of any VC produced, or possibly direct aerobic oxidation of *cis*-DCE

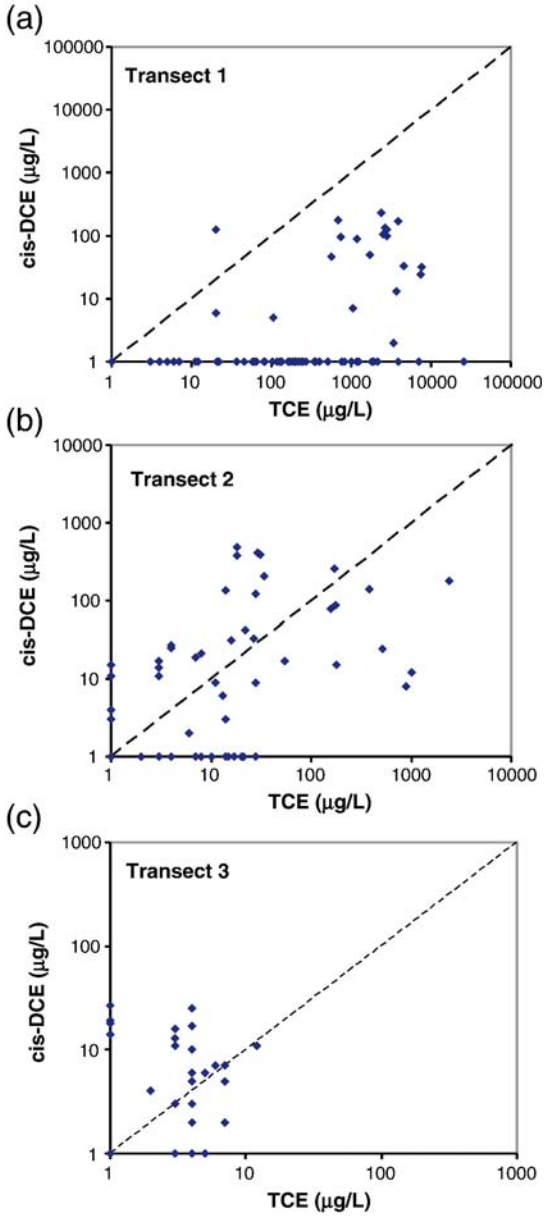

Fig. 10. Scatter plots showing TCE versus *cis*-DCE for samples from (a) Transect 1, (b) Transect 2 and (c) Transect 3 from August 2000.

which would not produce VC (e.g. Wiedemeier et al., 1999; Chapelle, 2001). Direct aerobic oxidation of *cis*-DCE and/or VC may occur where aerobic conditions exist near pond/stream interfaces with groundwater. Hydrogeochemical monitoring of the aquifer and compound-specific carbon isotope analyses were conducted to acquire evidence concerning whether complete dechlorination may contribute to the observed strong plume attenuation.

4.5.1. Hydrogeochemical conditions

Hydrogeochemical conditions at selected multilevels along the transects and piezometer nests between transects (Table 1) show consistency with the observed distributions of TCE and degradation products. Along Transect 1 (ML-10) conditions are aerobic with nitrate and sulfate present, very low dissolved iron and manganese (mostly below MDLs) and negligible DOC. These conditions are not supportive of reductive dechlorination (e.g. Wiedemeier et al., 1999; Chapelle, 2001), and are consistent with minimal TCE transformation to *cis*-DCE between the source and Transect 1. "Background" chloride values along Transect 1 were in the 10s of mg/L, suggesting chloride increases would not be a useful indicator of reductive dechlorination (e.g. complete dechlorination of 5000 μg/L of TCE would produce about 4000 μg/L of chloride, likely too small to be distinguished from background levels). Along the lower terrace, conditions are more amenable for reductive dechlorination, presumably due to input of natural DOC given the near surface position of the water table and natural soil cover (forested/wetland/grassy areas). Beyond the base of the embankment close to x-stream at DP-2 (Fig. 3), DO was low (<1 mg/L, possibly anaerobic), nitrate was very low to non-detect, dissolved iron and manganese were detected (maximum of 1.4 and 0.3 mg/L, respectively) and redox potential was the most reducing measured along the plume flowpath (−360 mV, uncorrected). Methane was also detected (up to 970 μg/L) along with traces of ethane and ethene. DOC was also observed in the 1–3 mg/L range. These highly reducing methanogenic conditions are consistent with TCE transformation to *cis*-DCE and further to VC (detected only at locations near the base of the embankment) with complete dechlorination possible (Chapelle, 2001). Along Transect 2 (ML-16) conditions were less amenable to reductive dechlorination, although only one location was investigated. DO was low but up to 1.5 mg/L, representing either marginally aerobic or anaerobic conditions. Nitrate was present (~1 mg/L), redox potential was less reducing than observed upgradient at DP-2 and methane was detectable but very low (5–15 μg/L). DOC was also lower (close to MDLs). Between Transects 2 and 3 (DP-5; Fig. 3) conditions were again more amenable to reductive dechlorination. DO levels were low (<0.5 mg/L) and nitrate was non-detect except at the shallow point (0.3 mg/L). DOC ranged from 1.6 to 1.8 mg/L and methane was detected in all points (600 to 1100 μg/L) along with traces of ethane (<1 μg/L) and ethene (<25 μg/L). Along Transect 3 next to the stream (ML-17), two shallower points provided very different results from deeper points, presumably due to stream influence. River levels were high at the time of sampling, so the stream was likely losing to the groundwater system near the river. The two shallow points were aerobic with nitrate present and lower sulfate and chloride than observed elsewhere. In contrast, the two deeper points showed conditions more suitable for reductive dechlorination, with low DO (<1 mg/L), nitrate below detection, DOC in the range of 1.6 to 1.8 mg/L and methane present (80–190 μg/L).

Hydrogeochemical monitoring confirms conditions along the lower terrace are favorable for reductive dechlorination, whereas upgradient conditions between the source zone and Transect 1 are not. This is consistent with the distribution of TCE and *cis*-DCE along the transects (Figs. 4 and 5) and the scatter plots (Fig. 10), showing transformation of remaining TCE to *cis*-DCE along the lower terrace in the groundwater. VC was only observed near the base of the embankment where reducing conditions were strongest, and not further downgradient along Transects 2 and 3. Input of natural organic carbon along the lower terrace appears to be a key factor causing the reducing conditions and providing hydrogen necessary for reductive dechlorination. Accumulation of *cis*-DCE and VC is minimal, with maximum *cis*-DCE concentrations near the river along Transect 3 in the tens of μg/L (Figs. 5c and 10c) and no VC observed, suggesting complete degradation may be one of the contributors to plume mass loss. This is examined further using compound specific isotope data.

Table 1
Results of hydrogeochemical sampling along the plume flow path

Sample ID	Depth (m bgs)	Chlorinated VOCs (µg/L)			Field parameters					Inorganics (mg/L)					Hydrocarbons (µg/L)			DOC
		TCE	*cis*-DCE	VC	pH	Redox potential (mV)	Electrical conductance (µS/cm)	Alkalinity (mg/L as $CaCO_3$)	DO (mg/L)	Cl	NO_3 (as N)	SO_4	Fe	Mn	Methane	Ethane	Ethene	(mg/L)
	MDL	1	100	n/a	–	–	–	–	–	1.0	0.05	2	0.02	0.01	0.3	0.2	0.2	0.5
Transect 1																		
ML10-2	7.8	27	<mdl	–	6.22	−38	288	6	5.7	37.0	2.0	15	<mdl	<mdl	<mdl	<mdl	<mdl	<mdl
ML10-4	9.1	196	<mdl	–	5.86	−39	286	17	0.6	41.3	2.1	16	<mdl	<mdl	<mdl	<mdl	<mdl	<mdl
ML10-6	10.5	691	<mdl	–	5.84	−37	294	17	0.5	40.9	2.0	17	<mdl	<mdl	<mdl	<mdl	<mdl	<mdl
ML10-8	11.1	4717	<mdl	–	6.16	−71	364	25	1.5	40.8	1.7	16	<mdl	0.02	<mdl	<mdl	<mdl	<mdl
ML10-9	11.4	5868	<mdl	–	6.38	−135	338	34	1.1	40.5	1.6	16	0.03	0.14	<mdl	<mdl	<mdl	<mdl
Between transects 1 and 2																		
DP2-b	1.2	<mdl	<mdl	–	6.67	−357	413	23	0.5	53.7	<mdl	26	1.41	0.28	158	4.5	<mdl	2.8
DP2-c	2.1	2205	302	–	6.70	−366	364	25	1.0	43.0	0.4	15	0.09	0.10	966	2.3	0.4	0.8
Transect 2																		
ML16-4	2.8	494	<mdl	–	6.07	−173	340	19	0.6	39.7	1.2	20	0.05	0.14	5	<mdl	<mdl	<mdl
ML16-5	3.2	532	184	–	6.43	−244	319	31	1.4	39.4	1.1	17	0.37	0.47	15	<mdl	<mdl	0.6
Between transects 2 and 3																		
DP5-a	1.5	49	<mdl	–	6.51	−221	535	27	0.3	69.8	0.3	29	0.02	0.13	597	0.8	15.3	1.8
DP5-b	2.1	85	<mdl	–	6.77	−202	547	34	0.2	69.1	<mdl	30	0.02	0.10	1091	0.4	<mdl	1.6
DP5-c	3.0	130	<mdl	–	6.81	−180	517	46	0.4	65.7	<mdl	20	0.03	0.18	1013	<mdl	24.5	1.6
Transect 3																		
ML17-1	1.4	1	<mdl	–	6.44	−160	210	39	4.8	7.6	0.7	14	0.03	0.01	7	<mdl	<mdl	0.6
ML17-3	2.0	1	<mdl	–	6.26	−100	192	32	8.0	7.5	0.9	10	0.04	<mdl	<mdl	<mdl	<mdl	0.8
ML17-5	2.6	40	<mdl	–	5.91	−218	490	25	0.5	68.0	<mdl	46	0.03	0.70	77	<mdl	<mdl	1.6
ML17-7	3.2	42	<mdl	–	5.95	−170	525	28	0.9	67.4	<mdl	47	0.03	0.65	189	<mdl	<mdl	1.8

Locations sampled are shown in Fig. 3.

4.5.2. Compound specific carbon isotopes

TCE and *cis*-DCE $\delta^{13}C$ values from the three transects fall within a narrow range. Along Transect 1 $\delta^{13}C$ values for TCE range from −22.6 to −21.6‰ with an average of −22.2‰ (11 samples), similar to source zone groundwater (32 samples, range −22.5 to −21.4‰ with an average $\delta^{13}C$ value of −22.0‰) and DNAPL (−21.8‰) provided by Hunkeler et al. (2003). $\delta^{13}C$ values for *cis*-DCE in the few samples where it was detected were similar to TCE (4 samples, range −22.9 to −22.5‰). Assuming *cis*-DCE degradation has not occurred to this point, which is reasonable given hydrogeochemical conditions and VC absence along Transect 1, the small difference between TCE and *cis*-DCE ratios suggests a small isotope enrichment factor for TCE degradation at this site. Along Transect 2, $\delta^{13}C$ values for TCE (8 samples, range −22.0 to −17.0‰, average −21.1‰) show a small average enrichment of +1.3‰ compared to Transect 1, with one sample downgradient of the pond (ML32-5) showing a larger enrichment of +5.2‰. Such shifts are at the low end observed in lab microcosm studies of microbial TCE degradation (e.g. Bloom et al., 2000) and appear consistent with the amount of TCE to *cis*-DCE transformation indicated by contaminant distributions (Figs. 4b and 5b) and compound ratios (Fig. 10b) along Transect 2. A similar small ^{13}C enrichment for *cis*-DCE (7 samples, range −21.9 to −20.6‰, average −21.2‰) of +1.4‰ on average was observed along Transect 2. Much larger shifts have been observed in lab and field studies where *cis*-DCE degradation occurs (e.g. Hunkeler et al., 1999; Bloom et al., 2000) suggesting minimal *cis*-DCE degradation occurs between Transects 1 and 2. However, the Transect 2 data is affected by groundwater discharge and mixing within the pond and interactions with x-stream and larger shifts in *cis*-DCE isotope ratios were observed in upgradient piezometer nests (see below). Along Transect 3, $\delta^{13}C$ data for both TCE (7 samples, range −22.2 to −20.9‰, average −21.8‰) and *cis*-DCE (6 samples, range −22.6 to −20.7‰, average −22.0‰) did not show evidence of further carbon isotope shifts, suggesting minor VOC degradation between Transects 2 and 3.

Much larger shifts in $\delta^{13}C$ (range from −13.8 and −18.4‰) for *cis*-DCE compared to Transect 2 were observed in piezometer nests between Transects 2 and 3 (DP-5 and PN-3; Fig. 3), suggesting *cis*-DCE degradation occurs locally within or upgradient of this portion of the plume and is spatially variable. Results of hydrogeochemical sampling at DP-5 (discussed earlier) confirm conditions suitable for *cis*-DCE degradation in this area. The largest isotopic shifts were observed at piezometer nests DP-1, DP-4 and PN-4 (Fig. 11) located near the base of the embankment and just upgradient of the pond (Fig. 3). TCE carbon isotope ratios were only marginally enriched compared to Transect 1 (range from −19.6 to −22.0‰) but large $\delta^{13}C$ shifts (range from −24.0 to +6.2‰) were observed for *cis*-DCE. The most enriched $\delta^{13}C$ values for *cis*-DCE were observed in shallow piezometers occurred at DP-1 (+6.2‰) and PN-4 (−0.1‰) (Fig. 11), indicating significant transformation of *cis*-DCE in this area, consistent with VC detections in August 2000 (Figs. 7a and 8a). These results suggest that occurrence of degradation is very location and depth specific. While there is clear evidence for degradation immediately upgradient of the pond, two samples from the pond (SW-22, SW-23; Fig. 3) showed only minor $\delta^{13}C$ shifts for TCE (−21.7 and −21.6‰, respectively) and *cis*-DCE (−20.5 and −20.2‰). This is attributed to effects of mixing and spatial variability, since some groundwater discharging to the pond would have isotopic signatures showing significant degradation (as observed in some piezometer nest points) but mixing with groundwater showing only minor degradation dampens the isotopic shifts observed in the pond. It is also important to note that isotope sampling was conducted in December, when degradation rates may have been lower due to lower temperatures, particularly near groundwater–surface water interfaces.

The relative enriched $\delta^{13}C$ values observed in piezometers nests near the base of the embankment did not persist downgradient along Transect 2, nor did the enriched values observed at piezometer nests between Transects 2 and 3 persist along Transect 3. This is likely due to loss of the groundwater

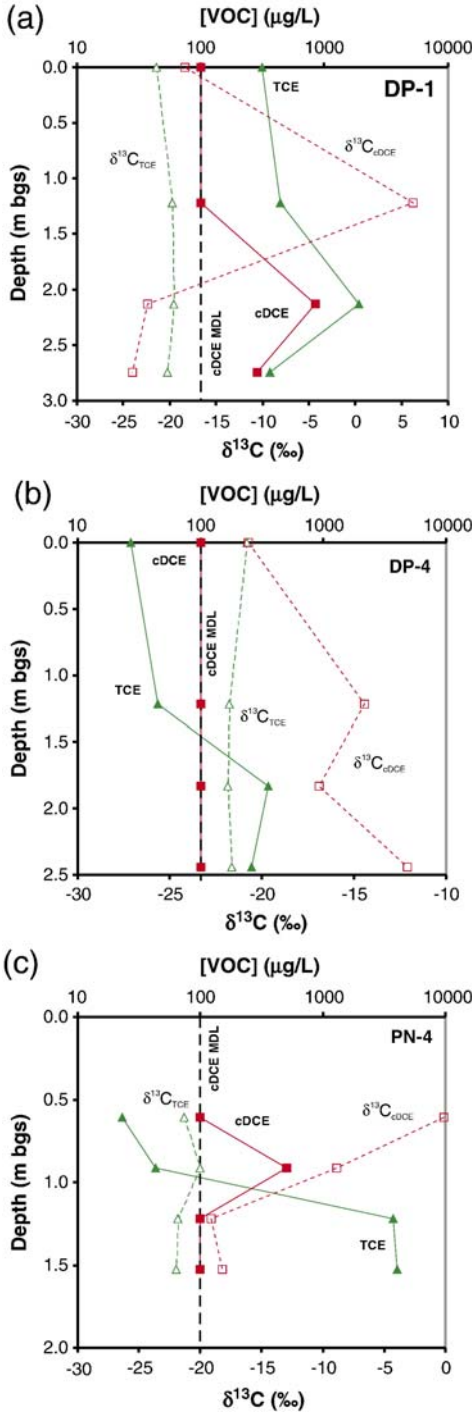

Fig. 11. Plots showing VOC concentrations and carbon isotope ratios from December 2000 sampling episode at piezometers near the base of the embankment and upgradient of the pond: (a) DP-1, (b) DP-4 and (c) PN-4.

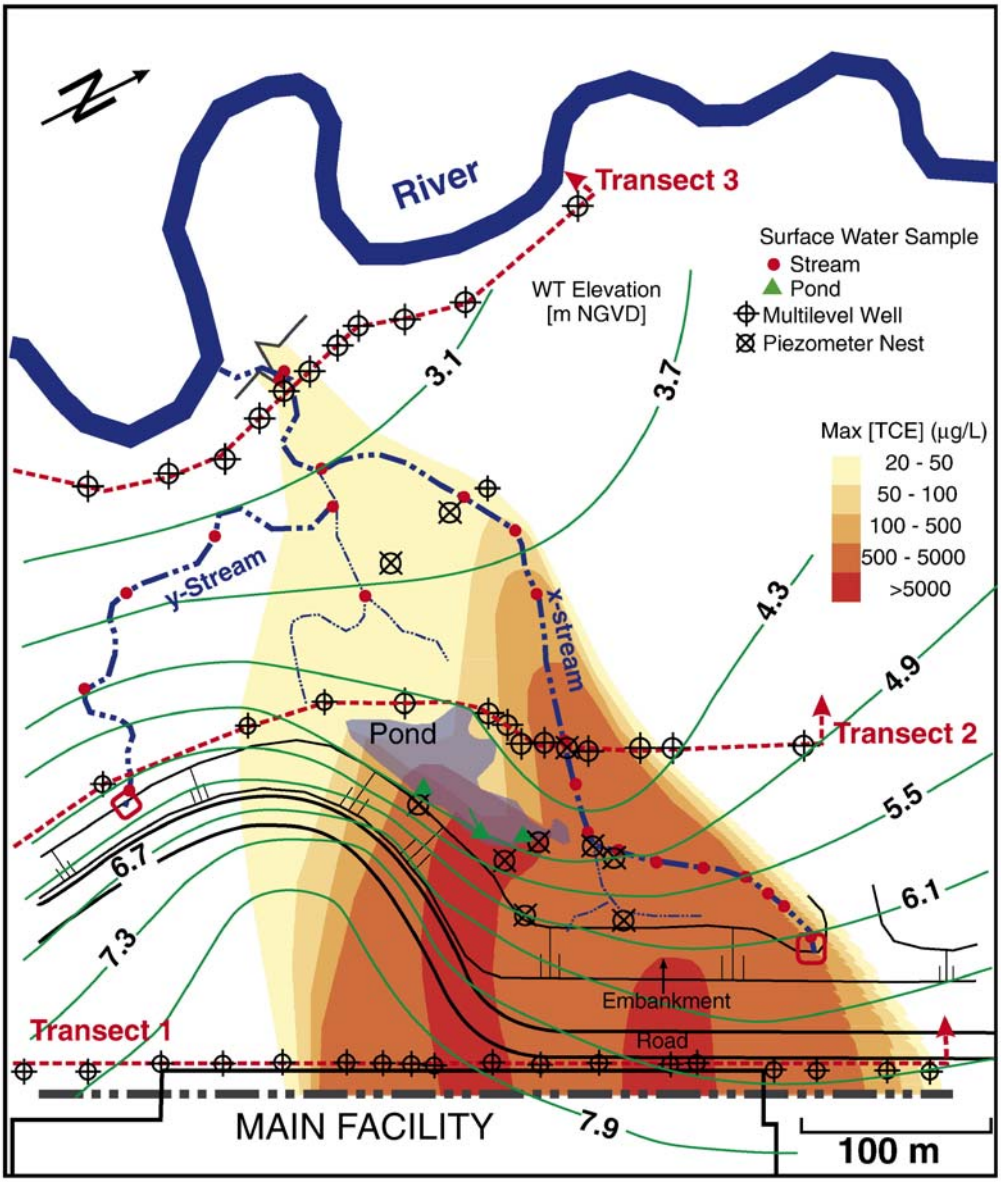

Fig. 12. Maximum plan view TCE concentrations in groundwater observed during this study in multilevels and piezometer nests. Water table contours (September 1999) are also shown.

plume to surface water (pond, streams) where mixing of groundwater with different isotope ratios, dilution and mass transfer to the atmosphere occur, allowing the groundwater to retain the less enriched $\delta^{13}C$ values ratios seen upgradient of the pond. However, clear evidence of *cis*-DCE degradation was provided by isotope data from the piezometer nests near the base of the embankment and upgradient of the pond, and between Transects 2 and 3. The lack of VC along Transect 2 or further downgradient may be interpreted that any VC produced from *cis*-DCE degradation also

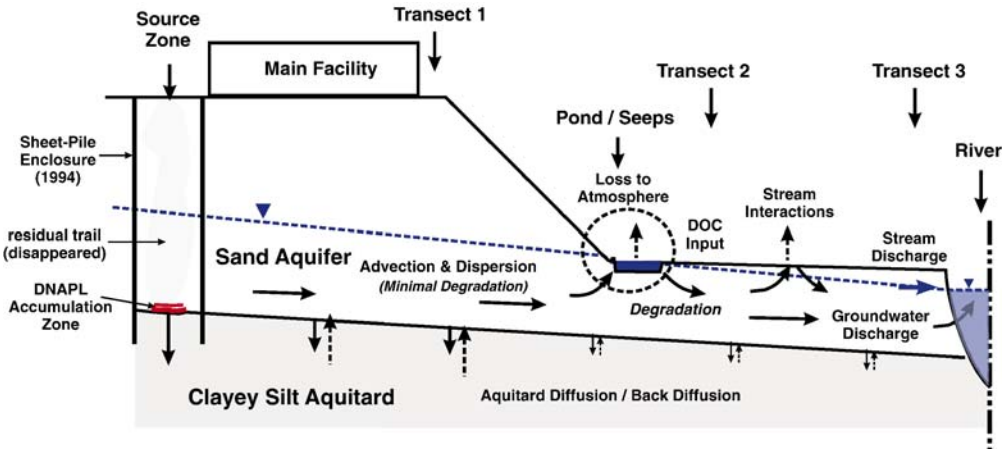

Fig. 13. Conceptual representation of VOC mass transport and attenuation pathways.

degrades given the strongly reducing (methanogenic) conditions in some areas. Another possibility is that VC and/or *cis*-DCE degrades by direct aerobic oxidation (Chapelle, 2001), given aerobic conditions in or near the surface water environment (pond/streams). It is also possible that physical mechanisms (discharge to and dilution in the pond and streams and loss to the atmosphere) cause loss of VC, so concentrations remained below the elevated MDLs. More study would be required to conclusively prove whether complete degradation is occurring, to quantify the amount of mass loss via complete degradation, mechanisms for such degradation and spatial and temporal variability. In any case, VOC distributions, aquifer hydrogeochemical conditions and carbon isotope data clearly show evidence of transformation of TCE and *cis*-DCE, and suggest that some complete degradation may be occurring, which contributes to the observed strong plume attenuation.

5. Conclusions

At the study site, detailed transect monitoring shows a decline of the maximum TCE concentrations in the groundwater plume by three orders of magnitude and TCE mass discharge from more than 100 to <0.5 g/day over a 420 m travel distance, prior to the plume discharging to the river via groundwater flow. Although, these results show strong apparent TCE attenuation in the groundwater zone, they would be misinterpreted if the influences of groundwater–surface water interactions are not taken into account. The maximum plan-view TCE concentrations in groundwater observed during this investigation (Fig. 12) highlights the impact of groundwater–surface water interactions on the plume, particularly the truncation of high concentrations in the southern portion of the plume by the pond, and the influence of x-stream on the portion of the plume passing to the north of the pond as it migrates toward the river. Fig. 13 is a schematic representation of the VOC attenuation (mass loss) and mass flux pathways for the site.

The investigation of groundwater–surface water interaction indicates that, although only very small plume VOC mass discharge enters the river via groundwater seepage, roughly half of the plume mass discharge crossing Transect 1 enters the river directly via small streams receiving groundwater discharge east of the river; hence, the importance of mass discharge estimates. The other half is apparently lost from the hydrologic system by mass transfer from surface water (pond, streams, seeps) to the atmosphere and by degradation. The occurrence of degradation is supported by

VOC distributions, hydrogeochemical conditions and compound-specific carbon isotope data, indicating that both TCE and *cis*-DCE degrade. Although it is unknown whether much VOC mass is lost by complete dechlorination, such loss likely occurs locally. Occurrence of reductive dechlorination may be largest during plume discharge through organic-rich near surface sediments and bottom sediments in the pond and streams. Although the river receives TCE and degradation products from the groundwater zone and streams, these contaminants are not detected in the river due to dilution. If natural attenuation is defined as the concentration decline due to subsurface processes, not through mass transfer out of the groundwater system, then this aquifer shows relatively weak attenuation capacity. The majority of the apparent groundwater plume attenuation occurs through plume mass discharge to surface water receptors, where the mass is well-attenuated by dilution, mass transfer to the atmosphere, and to some extent by degradation.

Acknowledgements

The field and laboratory analytical data reported on in this paper resulted from the skillful work of several University of Waterloo staff: in the field, Robert Ingleton, Jesse Ingleton, Paul Johnson, Hester Groenevelt, Daryl Bassett, Bryn Shurmer, Matt Nelson, Martin Guilbeault, Colin Meldrum and David Thomson; and in the lab, Maria Gorecka, Daryl Bassett and Hester Groenevelt. Daniel Hunkeler, now at the University of Neuchâtel, performed the compound-specific carbon isotope analyses. The Organic Geochemistry Lab at the University of Waterloo performed the dissolved hydrocarbon and TOC/DOC analyses. Lisa Akers, Erin MacDonald-Sullivan and Lauren Levine of United Technologies Corporation provided essential on-site support for field activities and stream discharge data. Rob Danielson of Fuss and O'Neill Inc. provided water level data and other useful site information. The manuscript was much improved as a result of the journal review process and careful reviews by two anonymous reviewers and the Editor Dr. Poul Bjerg. Funding for this research was provided by United Technologies Corporation and the University Consortium Solvents-in-Groundwater Research Program.

References

Avery, C., 1994. Interaction of ground water with the Rock River near Byron, Illinois. U.S. Geol. Surv. Water Res. Invest. Rep. 94, 4034.

Barker, J.F., Belland-Pelletier, C., Blaine, F., Devlin, J.F., King, M.W.G., Schirmer, M., 2000. Monitored natural attenuation: can mass flux through monitoring fences document mass loss in groundwater plumes? Proceedings of the International Conference on Groundwater Research, Groundwater 2000, Copenhagen, Denmark, June 6–8, 2000. A.A. Balkema, Rotterdam, Netherlands.

Benker, E., Davis, G.B., Barry, D.A., 1997. Factors controlling the distribution and transport of trichloroethene in a sand aquifer: hydrogeology and results of an in situ transport experiment. J. Hydrogeol. 202, 315–340.

Bloom, Y., Aravena, R., Hunkeler, D., Edwards, E., Frape, S.K., 2000. Carbon isotope fractionation during microbial dechlorination of trichloroethene, *cis*-1,2-dichloroethene, and vinyl chloride: implications for assessment of natural attenuation. Environ. Sci. Technol. 34 (13), 2678–2772.

Chapelle, F.H., 2001. Ground-Water Microbiology and Geochemistry, 2nd ed. John Wiley and Sons, Inc., New York.

Chapman, S.W., Parker, B.L., 2005. Plume persistence due to aquitard back-diffusion following DNAPL source removal or isolation. Water Resour. Res. 41 (12), W12411.

Cherry, J.A., 1997. Conceptual models for chlorinated solvent plumes and their relevance to intrinsic remediation. Proceedings of the Symposium on Natural Attenuation of Chlorinated Organics in Ground Water, Dallas, Texas, Sept. 11–13, 1996, United States Environmental Protection Agency, EPA/540/R-97/504, pp. 31–32.

Cherry, J.A., Parker, B.L., 1997. Field studies of solvent plume characteristics in sandy aquifers using profile sampling techniques. Proceedings 1997 International Conference on Groundwater Quality Protection: Remedial Technology and Management Policy for NAPL Contamination, Taipei, Taiwan, December 1–3, pp. 15–22.

Cherry, J.A., Gillham, R.W., Anderson, E.G., Johnson, P.E., 1983. Hydrogeological studies of a sand aquifer at an abandoned landfill: 2. Groundwater monitoring devices. J. Hydrol. 63 (1), 31–49.

Conant Jr., B., Cherry, J.A., Gillham, R.W., 2004. A PCE groundwater plume discharging to a river: influence of the streambed and near river zone on contaminant distributions. J. Contam. Hydrol. 73, 249–279.

Dempster, H.S., Sherwood Lollar, B., Feenstra, S., 1997. Tracing organic contaminants in groundwater: a new methodology using compound-specific isotopic analysis. Environ. Sci. Technol. 31, 3193–3197.

Einarson, M.D., 1995. Enviro-Core, a new direct-push technology for collecting continuous soil cores. Proceedings of the Ninth National Outdoor Action Conference and Exposition, Aquifer Remediation/Ground Water Monitoring/ Geophysical Methods, May 2–4, 1995, Las Vegas, Nevada.

Einarson, M.D., Mackay, D.M., 2001. Predicting impacts of groundwater contamination. Environ. Sci. Technol. 35 (3), 66A–73A.

Einarson, M.D., Cherry, J.A., 2002. A new multilevel ground water monitoring system using multichannel tubing. Ground Water Monit. Remediat. 22 (4), 52–65.

Casey, M.B., Winglewich, D.L., Morkin, M.I., 1998. Enviro-Core — a dual-tube direct push system for rapid site characterization. Proceedings of the Symposium on the Application of Geophysics to Environmental and Engineering Problems (SAGEEP), March 1998, Chicago, Illinois, pp. 1–10.

Engelen, G.B., Kloosterman, F.H., 1996. Hydrological Systems Analysis: Methods and Applications. Kluwer Academic Publishers, Dordrecht, The Netherlands. 152 pp.

Górecki, T., Pawliszyn, J., 1997. Field-portable solid-phase microextraction/fast GC system for trace analysis. Field Anal. Chem. Technol. 1 (5), 277–284.

Guilbeault, M.A., Parker, B.L., Cherry, J.A., 2005. Mass and flux distributions from DNAPL zones in sandy aquifers. Ground Water 43 (1), 70–86.

Harrington, R.R., Poulson, S.R., Drever, J.I., Colberg, P.J.S., Kelly, E.F., 1999. Carbon isotope systematics of monoaromatic hydrocarbons: vaporization and adsorption experiments. Org. Geochem. 30, 765–775.

Hess, E.C., Parks, J.H., Cook, J.K., 1989. The application of seepage meter technology to the monitoring of hazardous waste sites. Proceedings of the Conference on Hazardous Waste Research, Manhattan, Kansas, May 23–24, pp. 358–367.

Huang, L., Sturchio, N.C., Abrajano Jr., T., Heraty, L.J., Holt, B.D., 1999. Carbon and chlorine isotope fractionation of chlorinated aliphatic hydrocarbons by evaporation. Org. Geochem. 30, 777–785.

Hunkeler, D., Aravena, R., Butler, B.J., 1999. Monitoring microbial dechlorination of tetrachloroethene (PCE) in groundwater using compound-specific stable carbon isotope ratios: microcosm and field studies. Environ. Sci. Technol. 33, 2733–2738.

Hunkeler, D., Aravena, R., Parker, B.L., Cherry, J.A., Diao, X., 2003. Monitoring oxidation of chlorinated ethenes by permanganate in groundwater using stable isotopes: laboratory and field studies. Environ. Sci. Technol. 37, 798–804.

Hunkeler, D., Chollet, N., Pittet, X., Aravena, R., Cherry, J.A., Parker, B.L., 2004. Effect of source variability and transport processes on carbon isotope ratios of TCE and PCE in two sandy aquifers. J. Contam. Hydrol. 74, 265–282.

Kampbell, D.H., Wilson, J.T., Vandergrift, S.A., 1989. Dissolved oxygen and methane in water by GC headspace equilibration technique. Int. J. Environ. Anal. Chem. 36, 249–257.

Lorah, M.M., Olsen, L.D., 1999. Natural attenuation of chlorinated volatile organic compounds in a freshwater tidal wetland: field evidence of anaerobic biodegradation. Water Resour. Res. 35 (12), 3811–3827.

Meckenstock, R.U., Morasch, B., Grienler, C., Richnow, H.H., 2004. Stable isotope fractionation analysis as a tool to monitor biodegradation in contaminated aquifers. J. Contam. Hydrol. 75 (3–4), 215–255.

National Research Council, 2000. Natural Attenuation for Groundwater Remediation. National Academy Press, Washington, D.C.

Norman, W.R., Ostrye, D.P., Hobin, J.S., 1986. Use of seepage meters to quantify groundwater discharge and contaminant flux into surface water at the Baird and McGuire site. Proceedings of the Third Annual Eastern Regional Ground Water Conference, Springfield, MA, July 28–30. National Water Well Association, Dublin, OH, pp. 472–493.

Parker, B.L., Cherry, J.A., Chapman, S.W., Guilbeault, M.A., 2003. Review and analysis of chlorinated solvent dense nonaqueous phase liquid distributions in five sandy aquifers. Vadose Zone J. 2, 116–137.

Parker, B.L., Cherry, J.A., Chapman, S.W., 2004. Field study of TCE diffusion profiles below DNAPL to assess aquitard integrity. J. Contam. Hydrol. 74, 197–230.

Pawliszyn, J., 1997. Solid Phase Microextraction: Theory and Practice. Wiley, New York.

Pitkin, S.E., Cherry, J.A., Ingleton, R.A., Broholm, M., 1999. Field demonstrations using the Waterloo ground water profiler. Ground Water Monit. Remediat. 19 (2), 122–131.

Rathbun, R.E., 1998. Transport, behavior, and fate of volatile organic compounds in streams. U.S. Geol. Surv. Circ. 1589.

Schwarzenbach, R.P., Gschwend, P.M., Imboden, D.M., 2003. Environmental Organic Chemistry, 2nd ed. Wiley, Hoboken, NJ.

Sherwood Lollar, B., Slater, G.F., Ahad, J., Sleep, B., Spivack, J., Mackenzie, P., Brennan, M., 1999. Contrasting carbon isotope fractionation during biodegradation of trichloroethylene and toluene: implications for intrinsic bioremediation. Org. Geochem. 30 (8A), 813–820.

Sherwood Lollar, B., Slater, G.F., Sleep, B., Witt, M., Klecka, G., Harkness, M., Spivack, J., 2001. Stable carbon isotope evidence for intrinsic bioremediation of tetrachloroethene (PCE) and trichloroethene (TCE) at Area 6, Dover Air Force Base. Environ. Sci. Technol. 35, 261–269.

Slater, G.F., Dempster, H.S., Sherwood Lollar, B., Ahad, J., 1999. Headspace analysis: a new application for isotopic characterization of dissolved organic contaminants. Environ. Sci. Technol. 33, 190–194.

Slater, G.F., Ahad, J.M.E., Sherwood Lollar, B., Allen-King, R., Sleep, B., 2000. Carbon isotope effects resulting from equilibrium sorption of dissolved VOCs. Anal. Chem. 72, 5669–5672.

Slater, G.F., Edwards, E.A., Sleep, B., Sherwood Lollar, B., 2001. Variability in carbon isotopic fractionation during biodegradation of chlorinated ethenes: implications for field applications. Environ. Sci. Technol. 35, 901–907.

Squillace, P.J., Moran, M.J., Lapham, W.W., Price, C.V., Clawges, R.M., Zogorski, J.S., 1999. Volatile organic compounds in untreated ambient groundwater of the United States, 1985–1995. Environ. Sci. Technol. 33 (23), 4176–4187.

Stroo, H.F., Unger, M., Ward, C.G., Kavanaugh, M.C., Vogel, C., Leeson, A., Marqusee, J.A., Smith, B.P., 2003. Remediating chlorinated solvent source zones. Environ. Sci. Technol. 37 (11), 224A–230A.

Tóth, J., 1962. A theory of groundwater motion in small drainage basins in central Alberta. J. Geophys. Res. 67, 4375–4387.

Townley, L.R., Davidson, M.R., 1988. Definition of a capture zone for shallow water table lakes. J. Hydrol. 104, 53–76.

USEPA, 1991. Superfund NPL Characterization Project: National Results. U.S. Environmental Protection Agency, EPA/540/8–91/069.

Vroblesky, D.A., Lorah, M.M., Trimble, S.P., 1991. Mapping zones of contaminated ground-water discharge using creek-bottom-sediment vapor samplers, Aberdeen Proving Ground Maryland. Ground Water 29 (1), 7–12.

Vroblesky, D.A., Rhodes, L.C., Robertson, J.F., Harrigan, J.A., 1996. Locating VOC contamination in a fractured rock aquifer at the ground-water/surface-water interface using passive vapor collectors. Ground Water 34 (2), 223–230.

Westbrook, S.J., Rayner, J.L., Davis, G.B., Clement, T.P., Bjerg, P.L., Fisher, S.J., 2005. Interaction between shallow groundwater, saline surface water and contaminant discharge at a seasonally and tidally forced estuarine boundary. J. Hydrol. 302, 255–269.

Woessner, W.W., 2000. Stream and fluvial plain ground water interactions: rescaling hydrogeologic thought. Ground Water 38 (3), 423–429.

Winter, T.C., 1999. Relation of streams, lakes, and wetlands to groundwater flow systems. Hydrogeol. J. 7 (1), 28–45.

Winter, T.C., Harvey, J.W., Franke, O.L., Alley, W.M., 1998. Ground water and surface water — a single resource. U.S. Geol. Surv. Circ. 1139.

Wiedemeier, T.H., Rifai, H.S., Newell, C.J., Wilson, J.T., 1999. Natural Attenuation of Fuels and Chlorinated Solvents in the Subsurface. John Wiley and Sons Inc., New York. 617 pp.

Zapico, M.M., Vales, S.E., Cherry, J.A., 1987. A wireline piston core barrel for sampling cohesionless sand and gravel below the water table. Ground Water Monit. Rev. 7 (3), 74–82.

Zogorski, J.S., Carter, J.M., Ivahnenko, T., Lapham, W.W., Moran, M.J., Rowe, B.L., Squillace, P.J., Toccalino, P.L., 2006. The quality of our Nation's waters — volatile organic compounds in the Nation's ground water and drinking-water supply wells. U.S. Geol. Surv. Circ. 1292.